Supporting Information

30 Years of Advances in Functionalization of Carbon Nanomaterials for Biomedical Applications: A Practical Review

Neelkanth M. Bardhan

Department of Materials Science and Engineering, Department of Biological Engineering, Koch Institute for Integrative Cancer Research, Massachusetts Institute of Technology, Cambridge, MA 02139, USA.

Correspondence should be addressed to: bardhan@mit.edu or tweet the author: @Neel_Bardhan

Contents

1. Overview of the Properties of Fullerenes, Carbon Nanotubes and Graphene

The first CANOMAT to have been synthesized artificially was fullerene (occurring in carbon dust or soot, and later using laser evaporation of graphite), in the form of C_{60} by Kroto, H.W. *et al.*[1] Among the various zero-dimensional carbon nanomaterials explored since then, C_{60} remains the most widely investigated (although C_{70} is a close second), and shall form the primary focus for the purposes of this Review. The C_{60} molecule (also known as "bucky-ball" or "buckminsterfullerene") is a highly symmetrical truncated icosahedral structure, consisting of 12 pentagons and 20 hexagonal faces, with each vertex corresponding to a carbon atom. Each C atom is covalently bonded with 3 nearest neighbors. The structure has a van der Waals diameter ~ 1 nm, with a large volume of internal empty space, which has been exploited to place foreign atoms in this "molecular cage". Because of the icosahedral symmetry, this molecule is expected to show only four IR-active vibrational bands, proposed according to group theory, which we discuss in Figure S2(c). An interesting consequence of the high symmetry of this structure is that it has been reported[2] to show wave-like quantum interference – by far the largest and most massive single particle showing wave-particle duality. Further, the C_{60} molecule is extremely stable to high temperatures and pressures, with only surface reactivity of the carbon atoms without breaking open the geodesic dome structure.

Carbon nanotubes may be conceptualized as rolled-up cylinders of a single or a few layers of graphene[3], with a high aspect ratio (length : diameter) ~ $10^2 – 10^7$. The structure, diameter and electronic properties of a single-walled carbon nanotube (SWNT) are determined by the chiral vector (n, m)[4] (i.e. the vector along which the graphene sheet can be imagined to be rolled up, relative to the 2D lattice), as shown in Figure S1(a). Multi-walled carbon nanotubes consist of nested, concentric shells of SWNTs, with a spacing between individual walls of ~ 3.4 Å. Depending on the chiral vector, carbon nanotubes have differing electronic properties, with respect to the electronic band structure. These chiral vectors can be readily determined[5], for a given nanotube, through photoluminescence excitation (PLE) mapping. If $(n – m) = 3k$, the SWNTs are metallic; otherwise, they are semiconducting[6], i.e. there is a band gap between electronic states in the material. The latter are especially interesting from the point of view of making devices such as transistors, which depend upon switching states upon the application of a gate voltage; and for imaging probes involving optical band gaps, where the band-to-band transitions can be excited by means of an external stimulus. An example of the density of states is shown for a (6, 5) chiral semiconducting SWNT in Figure S1(c), calculated using real-space higher-order finite-difference pseudopotentials in a DFT implementation[7]. Aside from the unique opto-electronic properties, carbon nanotubes have also been predicted to possess exceptional mechanical properties, including very high specific strength ~ 48 MN·m/kg[8] (compared to only ~ 154 kN·m/kg for steel) and impact toughness (energy absorption capability)[9].

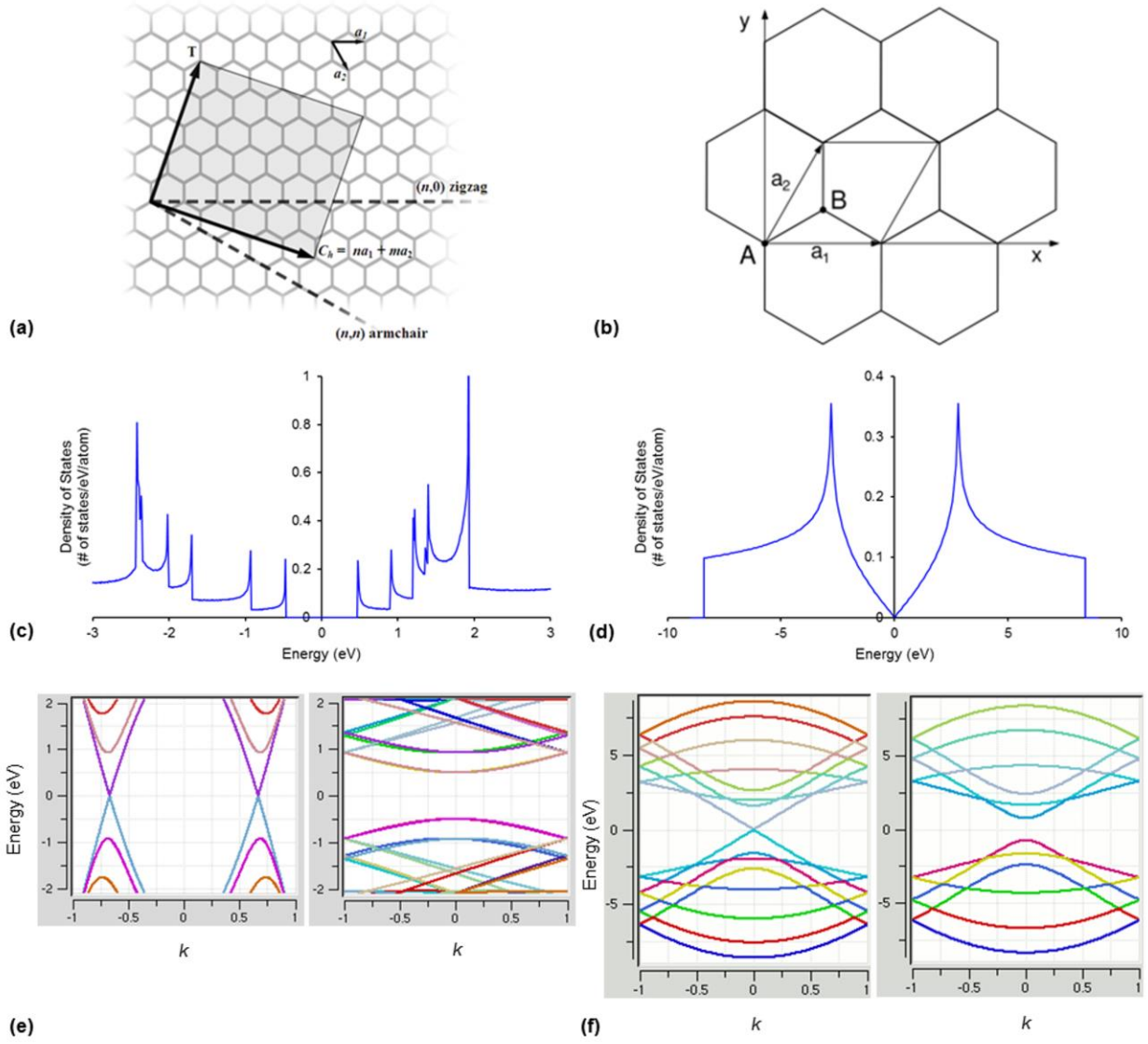

Figure S1: Basis set, electronic density of states, and energy dispersion diagrams for representative SWNTs and graphene nanoribbons.

(a) A schematic representation of the 2D carbon lattice, with the basis vectors $\overrightarrow{a_1}$ and $\overrightarrow{a_2}$, with the resulting rolling vector determining the chirality (*n*, *m*) by the linear combination $\overrightarrow{C_s} = n\overrightarrow{a_1} + m\overrightarrow{a_2}$. Also shown are two special cases of armchair (*n* = *m*) and zigzag (*m* = 0) oriented nanotubes. **(b)** The set of basis vectors $\overrightarrow{a_1}$ and $\overrightarrow{a_2}$ for the graphene lattice. **(c)** Representative density-of-states of a (6, 5) semiconducting SWNT, calculated using DFT. Note the presence of a band gap at 0 eV (the Fermi level). Typically, SWNTs absorb energies corresponding to the gap between the singularities in the density-of-states, relax through phonon-mediated transitions to lower gap levels, and emit fluorescence at longer NIR-II wavelengths. **(d)** Representative density-of-states of a (51, 51) graphene nanoribbon, calculated using a tight-binding approach within the Hückel approximation. At sufficient thicknesses of the nanoribbon, the graphene plane becomes a zero-gap conductor. **(e)** Electronic band structure of SWNTs, for *left* (10, 10) armchair metallic SWNTs, and *right* (2, 10) semiconducting SWNTs. **(f)** Energy dispersion diagrams of thin graphene nanoribbons, for *left* (8, 8) armchair metallic nanoribbons, and *right* (6, 6) armchair semiconducting nanoribbons. Zigzag-oriented graphene nanoribbons are always metallic. **(e, f)** Image rendered using nanoHUB tool[10].

Compared to fullerenes and carbon nanotubes, graphene is a recent addition to the family of carbon nanomaterials. Graphene is an atomically thin film of carbon, in a hexagonal lattice, with the atoms in an sp^2 hybridized state. The basis vector set for representing the graphene lattice is shown in Figure S1(b). the band structure, along with the electronic density-of-states, can be calculated for graphene using a tight-binding calculation using the Hückel approximation[11], the results of which are shown in Figure S1(d). Unlike semiconducting SWNTs shown in Figure S1(c), graphene is a zero-gap conductor, with group velocities which are similar to that of metallic SWNTs, leading to the observation of "ballistic" electronic transport over long range (~ μm) without significant scattering. Besides these unique opto-electronic properties, graphene and its derivatives are also very attractive due to the high carrier mobility, ~ 20,000 – 200,000 $cm^2/V/s$[12] (compared to only ~ 1,400 for silicon, the material of choice for current-generation electronics), superior thermal conductivity ~ 500 – 5,000 W/m/K[13] (compared to only ~ 400 W/m/K for copper, the material of choice for current thermal management solutions), ambipolar electric field effect[14], large surface area, high mechanical robustness with an intrinsic tensile strength ~ 130 GPa and Young's modulus ~ 1 TPa (compared to an ultimate tensile strength < 1 GPa for steel, the most common structural material), and the capability for chemical functionalization. It is not surprising, therefore, that this "material of the future" has piqued the intense curiosity of scientists, engineers and hobbyists worldwide.

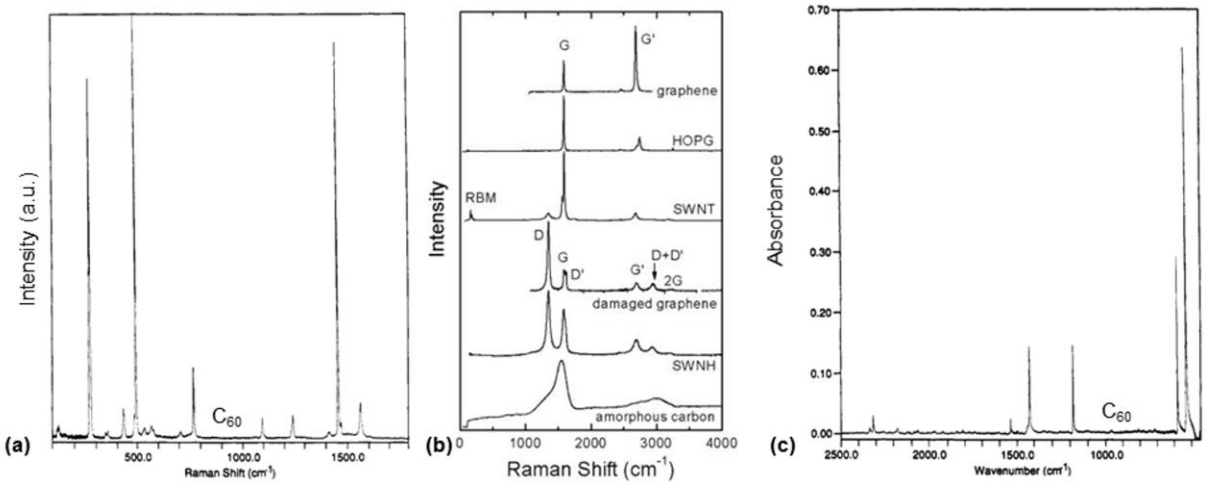

Figure S2: Characterization of CANOMATs using Raman and infrared spectroscopy.
(a) Raman spectrum of C_{60} thin film. **(b)** Raman spectra of various forms of sp^2 nanocarbons, including graphene, SWNT, damaged graphene, and amorphous carbon. **(c)** FTIR spectrum of C_{60} thin film.
(a, c) Reprinted (adapted) with permission from Chase, B. *et al.*[15] © 1992 American Chemical Society. **(b)** Reprinted (adapted) with permission from Dresselhaus, M.S. *et al.*[16] © 2010 American Chemical Society.

Before we delve into the methods of surface functionalization of CANOMATs for desired applications, it is important to be cognizant of the techniques used for identification and characterization of the "pristine" forms of these materials, so as to be able to identify the effect of functionalization. Raman spectroscopy has played an important role in the study of carbon-based materials, due to a strong Raman response, the relative simplicity of the spectra, and the

ease of access to this technique. Figure S2 presents Raman scattering spectra of (a) C_{60} and (b) a variety of 1D and 2D forms of carbon, including amorphous carbon. For C_{60} fullerene, only the eight 5-fold degenerate modes of H_g symmetry and the two non-degenerate modes of A_g symmetry are Raman active. The typical peaks assigned to the Raman spectra, shown in Figure S2(a), are[17]: 273.0, 432.5, 711.0, 775.0, 1101.0, 1251.0, 1426.5 and 1577.5 cm^{-1} for the H_g modes, and 497.5 and 1470.0 cm^{-1} for the A_g modes. These values are in good agreement with experimentally-predicted line values[18,19] of inelastic scattering. Further, Raman spectroscopy is even more important for carbon nanotubes and graphene, as it can provide information about the structure of the material, and the presence, if any, of defects or impurities. Referring to Figure S2(b), we note the presence of the *G*-band, which is attributed to the C–C bond stretching present in all sp^2-bonded carbon materials. For a 2D graphene sheet, a single peak is observed at ~ 1582 cm^{-1}, while there are multiple peaks, up to six, for chiral SWNTs, occurring due to curvature effects. The defect or disorder-induced *D*-band, on the other hand, is one of the most important ways to characterize the extent of disorder in CANOMATs. For example, Ar^+-ion bombardment creates point defects in a graphene sheet, which are manifested in the two *D*- and *D'*-bands at 1345 and 1626 cm^{-1}. The ratio of the intensities of the graphene and defect bands, I_D/I_G, is often used to quantify the extent of disorder, and is correlated to the size of graphitic domains in the structure[20]; especially for amorphous or disordered carbons. Next, we mention the presence of the *G'*-band, in the range of ~ 2500 – 2800 cm^{-1}, which is attributed to a second-order double resonance process. Unlike the other vibrational modes, this *G'*-band shows a strong dependence on the excitation frequency, and therefore, can appear in a range of wavenumbers. Further, the position of the *G'*-band can be used to distinguish the electronic structure, and the number of layers, the stacking order, and other scattering effects which are correlated to the number of Raman peaks. Moreover, SWNTs show a distinct *G'*-band, with the frequency and the number of peaks affected by the (*n*, *m*) chirality and curvature effects. In addition, there is a low frequency mode, typically in the range of 0 – 300 cm^{-1} for carbon nanotubes, called the Radial Breathing Mode (RBM). As the name suggests, this is a function of the radial vibration frequency, which is correlated to the diameter of the nanotubes, and the transition energies between the various states of the nanotubes. In the limiting case, for a tube with infinite diameter (graphene), the RBM frequency goes to infinity. Finally, in Figure S2(c) we discuss the use of FTIR spectroscopy to characterize these materials. An example is provided for C_{60} here; in general, absorption spectroscopy does not yield unequivocal identification results owing to the lack of heterogeneous chemical bonding in the pure forms of these CANOMATs, and therefore, inelastic Raman spectroscopy is the preferred technique. For a thin film of C_{60}, four main peaks are identified at 526, 576, 1183 and 1430 cm^{-1}, which point to the icosahedral structure of the molecule. While FTIR is certainly a useful tool for the study of surface-functionalized CANOMATs, and will be explored in the sections below, it does not find much use in the characterization of the pure forms of these materials. Although there have been FTIR studies[21] on carbon nanotubes and graphene, these studies take advantage of the impurities / adsorbed species resulting from the synthesis process of these materials, rather than being an intrinsic property of the material itself.

2. Review Parameters

The parameters used for this Review are as follows:

(1) Agent of Functionalization: This is the broad category of material which is being used as the functionalization technique, such as Polymer or DNA. In cases where there are sub-categories, they will be explored in further detail. For example, under the category of polymer-functionalized carbon nanotubes, we will list separate entries for PEG, M13 virus, or DNA, as various types of polymers.

(2) Number of Steps and Time required: This parameter looks into the number of steps necessary to functionalize the nanomaterial with the functionalization agent. Further, the time measures the actual amount of time necessary to implement the number of steps undertaken to functionalize the carbon nanomaterial with the functionalization agent. We do not account for the time required to synthesize, purify or prepare the functionalization agent (such as a polymer, which may be procured from a commercial vendor).

(3) Are any special instruments required? This aims to specify whether the functionalization technique requires special, expensive equipment such as chemical vapor deposition (CVD) reactors, which may not always be accessible to early-career researchers.

(4) Phase of functionalization: This lists the material forms in which the route of functionalization can be suitably used, i.e. whether it can be used in the bulk, thin film, powder, in suspension, or other forms, for greater diversity of applications.

(5) Properties affected: This lists the impact of the functionalization technique on the physical, chemical, electronic and optical properties of the CANOMAT. An attempt is made to distinguish the direction of the impact, whether positive or negative, with a qualifier for the magnitude (+, ++, +++ OR –, —, ——).

(6) Characterization techniques: The available methods for determining the properties and the extent of functionalization, such as SEM/TEM/AFM, XRD, XPS, IR/Raman spectroscopy, absorbance/emission/PL etc. are listed here.

(7) Scalability: This is an important criterion to consider, especially when developing applications for industrial use or clinical translation. It is rated on a (Low, Medium or High) scale, based upon the previous considerations of the need for special instruments, time or number of steps required to design the functionalized nanomaterial. In the cases of low scalability, an explanation is provided.

(8) Reproducibility: A crucial consideration is whether novel functionalization schemes reported in the literature have been successfully reproduced by others in the scientific community. This is broadly distinguished into General (i.e. the method has been reproduced by other research groups, distinct from the originator of the functional technology), Self (i.e. multiple instances of being reported by the same research group), or None (only one existing report of the functionalization technique). For this evaluation, we have performed a Google Scholar search of all the citations of the paper(s) under consideration, for a period of 5 years post publication. This metric indirectly provides a guide to the robustness of the technique.

(9) Applications: Finally, this comparison lists the most common applications for which this functionalization technique has been employed in the literature.

3. Additional Important routes to covalent functionalization of Fullerenes

3.1 Nucleophilic Addition

The reactivity of fullerenes is comparable to that of unsaturated carbon compounds, with ready attack by nucleophiles. Nucleophiles typically attach as 1,2-addition, but 1,4-addition is also reported in cases where steric hindrance plays a role, for the attachment of large moieties. Typical nucleophiles known to react with fullerenes are Grignard reagents, cyanide ion, organo-lithium derivatives, etc; resulting in open structures. In contrast, it has been shown possible to form 3-, 4-, 5- and 6-membered rings, respectively by 1,3-dipolar cycloaddition, [2 + 2] cycloaddition, [3 + 2] cycloaddition (such as the Prato reaction) or [4 + 2] cycloaddition. Another common reaction scheme is the Bingel cyclopropanation reaction, in which cyclopropane derivatives of C_{60} can be obtained by reacting with 2-bromomalonate esters, in the presence of a base such as NaH. For an excellent overview on the various reaction schemes available for the modification of fullerenes, refer to Prato, M.[22]

3.2 Hydrogenation of Fullerenes

Due to the presence of unsaturated double bonds, fullerenes are easily hydrogenated by various methods. Hydrofullerenes such as $C_{60}H_{18}$ and $C_{60}H_{36}$ have been reported, by the reaction of H_2 gas with fullerene at elevated pressure and temperature. However, at large concentrations, fully hydrogenated $C_{60}H_{60}$ is not considered to be stable due to strain in the cage structure, and this has been exploited as a method to unzip the cage structure to form hydrogenated nano graphene. The ability to react fullerenes with hydrogen has been exploited as a means to encapsulate hydrogen for hydrogen storage, as demonstrated by Komatsu, K. *et al*.[23]

Table 1: A summary of the comparison of functionalization schemes for fullerenes.
The metrics used for the comparison are described in the text in Section 2 above.
Phases: S (solid), L (liquid), G (gas), TF (thin film), aq. (aqueous medium)
Characterization techniques: SEM/TEM: Scanning / Transmission electron microscopy, PL: photoluminescence, UV-vis: Ultraviolet / visible absorbance spectroscopy, TGA: thermogravimetry analysis, XPS: X-ray photoelectron spectroscopy, NMR: nuclear magnetic resonance, AFM: atomic force microscopy, FTIR: Fourier Transform infrared spectroscopy, ICP-AES: inductively coupled plasma atomic emission spectroscopy

Agent of Functionalization	# of Steps (Time reqd.)	Special Equipment?	Phase of Func.	Properties affected (+/–)	Characterization Techniques	Scalable?	Reproducible?	Applications
Non-covalent Functionalization								
(1) Fullerene-macrocyclic complexes								
Porphyrin and its derivatives	1 (1 hr.)	Electrospray ionization	(Non-aq.) L, G	Energy transfer (+++)	MALDI-TOF	Medium	General[24]	Artificial photosynthesis[25]
Polymer-based composites: P3HT-PCBM	1 (1 hr.)	Spin coating, annealing	S (TF)	Energy transfer (+++)	Cyclic voltammetry, *I-V* curves, 4-point probe	High	General[26]	Organic photovoltaic devices such as polymer solar cells[27,28]
Covalent Functionalization								
(1) Addition Reactions								
Cycloadditions (1,3-dipolar, [2 + 2], [3 + 2] or [4 + 2], Bingel cyclopropanation)	1 (2 hr.)	No	L	Electron donor-acceptor interactions (+++), Ring opening, Encapsulation of other molecules, Water solubility (+++)	^{1}H-NMR, UV-vis	Medium	General[29]	Synthesizing unnatural amino acids such as fulleroproline[30] for peptide synthesis, anti-HIV and anti-bacterial activity[31]
(2) Hydrogenation, Oxidation and Hydroxylation								
Hydrogenation: reaction with H_2 gas	5 (> 36 hr.)	500W Xe lamp	S	Thermal stability (+++), color lightening (+), UV-vis absorbance (+)	^{1}H-NMR and ^{13}C-NMR, MALDI-TOF	Medium	General[32]	Hydrogen storage
Oxidation (using OsO_4, oxone monopersulfate, 3-chloroperoxy benzoic acid, O_3)	1 (6 - 12 hr.)	Vacuum drying, HPLC	L, G	Symmetry break	^{13}C-NMR, HPLC, XPS	Medium	General[33]	Non-obvious
Hydroxylation: "fullerenols" or "fullerols" (using dil. H_2SO_4 + KNO_3, or dil. NaOH + H_2O_2)	1 (5 days)	Dialyzer, freeze drying	L	Water solubility (+++)	^{13}C-NMR, FTIR, ICP-AES	Medium	General	Apoptotic cell cycle arrest[34] in cancer, preventing systemic toxicity in chemotherapy[35], delivery of hydrophobic drugs[36], gene delivery[37,38]
Gd@C_{60}: Metallofullerenes	2 (12 - 24 hr.)	Arc discharge chamber, HPLC	L	Hydrophilicity (+++), biodistribution (++)	MALDI-TOF, HPLC, Relaxometry	Medium	General[39]	MRI contrast agent[40–42], Tumor imaging and PDT[43,44]

4. Additional Important routes to covalent functionalization of Carbon Nanotubes

Disadvantages of small-molecule non-covalent functionalization of SWNTs

Despite their advantages in terms of ease of synthesis of the micellar-stabilized, aqueous-dispersed SWNT complex, small molecule surfactants are potentially highly toxic, and raise concerns for biomedical applications. This is further compounded by the presence of large excess of these small molecules in the dispersing medium (in order to maintain concentrations well above the CMC for the suspension to be stable), and the difficulty in preventing them from coating and potentially altering the activity of associated moieties such as targeting agents, drug molecules etc. Therefore, there has been tremendous ongoing effort to substitute these small molecule surfactants with other agents of functionalization, which we discuss in the following subsections.

4.1 Cycloaddition reactions

The first cycloadditions were performed by Chen, J. *et al*.[45] and Kamaras, K. *et al*.[46], by functionalization with octadecylamine (ODA), rendering the SWNTs soluble in organic solvents. These were synthesized by reacting dichlorocarbene generated *in situ* from $PhHgCCl_2Br$, to form carbon-carbon bonds to the sidewall of the CNT. In another approach, Georgakilas, V. *et al*.[47] have used 1,3-dipolar cycloaddition of azomethine ylides, generated by a condensation reaction between an α-amino acid and an aldehyde[48]. This reaction introduces approximately one organic group per 100 carbon atoms of the nanotube, with the resulting functionalized nanotube showing remarkable solubility (~ 50 μg/ml) in both water and organic solvents. Similarly, nitrenes can be introduced by [2 + 1] cycloaddition[49] to produce soluble SWNTs. Yinghuai, Z. *et al*.[50] have managed to attach substituted carborane cages to the sidewall of SWNTs using nitrene cycloaddition. One of these functionalized nanotubes was studied in an *in vivo* mouse model, bearing the structure $[Na^+][1\text{-}Me\text{-}2\text{-}((CH_2)_4NH\text{-})\text{-}1,2\text{-}C_2B_9H_{10}][OEt])_n$(SWNT), and it was reported that the boron atoms concentrate more in tumor cells than in blood and other organs (Figure 5(a) in the Main Text), making this a potential candidate for the delivery of boron for the use of boron neutron capture therapy in the treatment of cancer. In subsequent work, Dumortier, H. *et al*.[51] reported that SWNTs water-solubilized using the 1,3-dipolar cycloaddition reaction are uptaken by both B- and T-lymphocytes, as well as macrophages, and are not cytotoxic (neither did they induce cell death, nor affect lymphocytes' functionality, although they did evoke secretion of proinflammatory cytokines by macrophages, Figure 5(b) in the Main Text).

4.2 Halogenation reactions

Fluorination of SWNTs was first reported by Hamwi, A. *et al*.[52] and Mickelson, E.T. *et al*.[53], with the puckered tube-like structure of the functionalized SWNTs still maintained at reaction temperatures as high as 325 °C, up to a limiting stoichiometry of C_2F. The process of fluorination was investigated by Kudin, K.N. *et al*.[54], using DFT calculations and periodic boundary conditions. Their calculations (based on a C_2F stoichiometry) revealed that the addition of F atoms changes the local bonding environment of the respective carbon atoms, resulting in significant distortion to the pristine SWNT geometry. The fluorination of SWNTs can yield nanotube derivatives with different electronic properties (insulating, semiconducting or metallic), depending on the fluorination pattern. Fluorination has been commonly used by Gu, Z. *et al*.[55] and others, as a means to "cut" the SWNTs lengthwise, by high-temperature pyrolysis (1000 °C) following fluorination at a low stoichiometry CF_x ($x \leq 0.2$). At moderately high temperatures, (~ 100 - 400 °C), however, de-fluorination occurs, and it has been reported[56] that the functionalized SWNTs revert to clean SWNTs (rather than being etched), with no apparent change in the ratio of metallic : semiconducting tubes, with only a slight increase in the average tube diameter. In addition to fluorination, several other groups of researchers have tried chlorination[57,58] and bromination[59] of carbon nanotubes, with the formation of C–Cl or C–Br bonds respectively, with loading upto ~ 5 - 17% (by weight). In terms of applications, it has been proposed that cutting the fluorinated SWNTs greatly increases their surface area, with consequent advantages in terms of the ability to load and contain significant amount of tracers such as $^{125}I^-$ for radioimaging purposes[60]. In general, the use of reactions to attach halides on the sidewall results in severe defects which perturb the electronic structure of the carbon nanotubes, and therefore, they are not very well-suited for use in imaging applications.

4.3 Hydrogenation Reactions

As an alternative to oxidation, hydrogenation has also been explored as a means to introduce additional functionality to the sidewall of carbon nanotubes. In the first demonstration, Chen, Y. *et al*.[61] used Birch reduction to hydrogenate SWNTs, using either ammonia or ethylenediamine. The incorporation of C–H bonding was reported to cause change in the electronic structure of the tubes, owing to chemical disruption in the tube wall. The hydrogen bound to the carbon nanotubes is expected to be stable up to moderately high temperatures, ~ 400 - 500 °C[62]. Hydrogenation has been exploited as a mechanism for hydrogen storage (up to ~ 5% hydrogen capacity by weight, ~ 65% hydrogenation

of carbon atoms in the SWNT), such as that by Nikitin, A. *et al*.[63], as well as for etching (cutting) of SWNTs by Zhang, G. *et al*.[64] However, to the best of our knowledge, there have been no reported examples of the use of hydrogen-modified SWNTs for bio-applications.

Effect of Covalent Functionalization on Sidewall defects

Before we conclude the section on covalent functionalization of carbon nanotubes, it is worth pointing out one recent paper by Piao, Y. *et al*.[65] While the conventional wisdom has long held that the process of covalent functionalization introduces too many defects and causes perturbation in the electronic structure of SWNTs (by introducing dark trap states), thereby rendering them inefficient as contrast agents for imaging, the aforementioned group of researchers has challenged this hypothesis by clever band-gap engineering, while intentionally incorporating sp^3 defects into the sidewall structure of SWNTs. They demonstrated that the photoluminescence emission of the nanotubes can be brightened by ~ 28×, and could potentially lead to a method to harvest dark excitons in SWNTs, by the creation of allowed optical states in the E_{11} transition state through doping of the sp^3 defect sites. This new development has exciting implications for the ability to attach additional functional groups onto SWNTs through covalent conjugation chemistries, while still maintaining high near-IR fluorescence emission for *in vivo* imaging applications.

Table 2: A summary of the comparison of functionalization schemes for carbon nanotubes.
The metrics used for the comparison are described in the text in Section 2 above.
Phases: S (solid), L (liquid), G (gas), TF (thin film), aq. (aqueous medium)
Characterization techniques: SEM/TEM: Scanning / Transmission electron microscopy, PL: photoluminescence, UV-vis: Ultraviolet / visible absorbance spectroscopy, TGA: thermogravimetry analysis, XPS: X-ray photoelectron spectroscopy, NMR: nuclear magnetic resonance, AFM: atomic force microscopy, FTIR: Fourier Transform infrared spectroscopy, ICP-AES: inductively coupled plasma atomic emission spectroscopy

Agent of Functionalization	# of Steps (Time reqd.)	Special Equipment?	Phase of Func.	Properties affected (+/–)	Characterization Techniques	Scalable?	Reproducible?	Applications
Non-covalent Functionalization								
(1) Surfactants								
Charged small molecules: SDS, SC, NaDBBS, CTAB	4 (6 hr.)	Shear mixer, cup-horn sonicator, ultracentrifuge	L (aq.)	Purity (+++), Hydrophilicity (+++), Stability (+++), Photoluminescence (–)	UV-vis, PL, Raman, TEM	High	General[66]	Sorting of carbon nanotubes based on chirality[5], by diameter[67], or by electronic structure[68,69]
Nonionic Polymers: Tween, Triton-X, PVP, Pluronic	4 (6 hr.)	Shear mixer, cup-horn sonicator, ultracentrifuge	L (aq.)	Hydrophilicity (+++), Stability (+++), Photoluminescence (–)	UV-vis, PL, Raman, TEM	High	General[66]	Optical sensor for blood glucose detection[70], anti-bacterial solutions[71]
(2) Polymer-based functionalization								
Poly (Ethylene Glycol), PEG and its derivatives, phospholipid-PEG	2 (6 - 48 hr.)	Ultracentrifuge	L (aq.)	Hydrophilicity (+++), Stability (+++), Circulation life (+++)	TEM, UV-vis, PL	High	General[72]	Drug delivery[73], *in vivo* tumor targeting[74], NIR-II fluorescence imaging of tumor vasculature[75], high spatio-temporal resolution of hemodynamics[76], through-skull imaging of cerebral stroke[77], fluorescence angiography[78], simultaneous imaging and photothermal therapy[79]
M13-bacteriophage	1 (72 hr.)	Probe-tip sonicator, Ultracentrifuge	L (aq.)	Hydrophilicity (+++), Stability (+++), Photoluminescence (–), Signal-to-noise (+++)	TEM, UV-vis, PL	Medium	Self	NIR-II imaging of prostate cancer[80], ovarian cancer[81], bacterial infections[82]
DNA wrapping	2 (3 hr.)	Sonicator, Ultracentrifuge	L (aq.)	Hydrophilicity (+++), Stability (+++), Photoluminescence (–)	TEM, UV-vis, PL	Low	General[83]	Sorting of SWNTs based on length and chirality[84–87], *in vivo* optical detection of NO for inflammation[88,89] or other molecules like riboflavin[90], plant "nanobionics" for augmented photosynthesis[91]

Agent of Functionalization	# of Steps (Time reqd.)	Special Equipment?	Phase of Func.	Properties affected (+/–)	Characterization Techniques	Scalable?	Reproducible?	Applications
Covalent Functionalization								
(1) Direct Chemical Reactions								
Cycloaddition reactions (with octadecylamine, azomethine ylides, nitrene addition)	2 (3 - 12 hr., up to 5 days)	TLC/HPLC, Vacuum drying	S	Dispersion (+++), Band gap tenability (++), PL emission (–)	2D NMR, TGA, STM, TEM	High	General[92]	Boron delivery for neutron capture therapy in cancer[50], uptake by B- and T-cells[51]
Halogenation reactions (with HF, CHF_3, $CHCl_3$, C_2Cl_4, C_3F_6, CCl_4, Cl_2 gas or Br_2 solution)	1 (2 hr.)	Plasma chamber or high-T furnace with atm. control	S	Length cutting (+++), defects in sidewalls (—)	γ-ray emission, TEM, TGA, XPS	High	General[54]	Cutting of SWNTs[55], containment of radiotracers[60] such as $^{125}I^-$ for PET imaging
Oxidation (boiling HNO_3, H_2SO_4, "piranha", air or O_2/O_3 at high-temp., OsO_4, H_2O_2, $KMnO_4$, $K_2Cr_2O_7$) and Hydrogenation (Birch reduction: with NH_3 or $C_2H_4(NH_2)_2$ reactions)	1 (1 - 9 hr.)	Vacuum drying	L or G	Removal of metal catalyst impurities (+++), defects in sidewalls (—), length cutting (+/–), PL emission (——)	AFM, TEM, TGA, XPS, Raman	High	General[93]	Receptor-mediated endocytosis, efficient drug delivery[94–96], upregulating signaling with cell-specific immunostimulation[97], anticancer vaccine delivery[98], etching of SWNTs[64], high capacity (~ 5 wt.%) hydrogen storage[63]

5. Additional Important routes to functionalization of Graphene

5.1 Pyrene and its derivatives

The pyrene moiety has attracted great attention (Figure S3) due to its strong affinity to the graphene basal plane. For example, An, X. *et al.*[99] have demonstrated the non-covalent functionalization of graphene with pyrene carboxylic acid (PCA), and transferred the functionalized graphene films onto transparent poly-dimethylsiloxane (PDMS) substrates for optical and sensing applications (Figure S3(a)). The flexible, hybrid structure allows > 65% visible transmittance, while blocking up to 95% of the UV spectrum. This opens up new possibilities for designing optical filters for UV protection, such as in ophthalmology. In another approach, Xu, Y. *et al.*[100] have used a water-soluble pyrene derivative, 1-pyrenebutyrate, as a stabilizer. Using this non-covalent approach, they were able to disperse large-area graphene oxide sheets stably in water, and reported an improvement in the film conductivity by 7 orders-of-magnitude. This approach is useful for developing electrochemical sensors from chemically-derived graphene, which rely on the electronic conductivity of the graphene sheet for analyte detection.

Several groups of researchers have used derivatives of pyrene butanoic acid, such as the succidymidyl ester (PBASE) used by Wang, Y. *et al.*[101], or the succinimidyl ester (PYR-NHS) used by Kodali, V.K. *et al.*[102] While the former group mainly used it for improving the power conversion efficiency of photovoltaic devices (Figure S3(b)) using functionalized graphene to 1.71% compared to as-synthesized graphene, the latter group designed functionalized epitaxial few-layer graphene which can be micropatterned with immobilized proteins (Figure S3(c)) using contact printing. These modified graphene surfaces, with specific binding affinity to fluorescently labeled proteins, can be used for sensors such as those for monitoring glucose, cells, and tissue engineering applications. In a different application, Liu, Y. *et al.*[103] have used PBASE to form a self-assembled monolayer as a molecular "bridge" between layer-by-layer stacked CVD graphene sheets. Using this method, they were able to achieve an increase in the vertical inter-layer conductivity between the graphene sheets by up to 6 orders-of-magnitude, due to hole doping, orbital hybridization, planarization of the graphene sheets, and the exclusion of polymeric residues.

Another approach which has been used by several groups is to create composites of graphene with aromatic molecules which can act as electron donor and acceptor molecules. For example, Su, Q. *et al.*[104] have created graphene composites with tunable electronic properties, using pyrene and perylenediimide as the hole-conduction and electron-

conduction organic materials (Figure S3(d)). In addition to improving the stability of the aqueous dispersion of the graphene nanosheets, these molecules resulted in a dramatic increase in the conductivity, and consequently an increase in the power efficiency in heterojunction solar cells. In a similar manner, Cheng, H-C. *et al.*[105] have fabricated single-layer graphene *p-n* junctions by a resist-free, spatially-selective, microfluidic-delivered chemical modification process, using 1,5-diaminonaphthalene and 1-nitropyrene respectively as the electron- and hole-donating groups. Using this approach, field effect devices showed high carrier mobility, with minimal scattering and carrier degradation caused by the dopant molecules.

Recently, Papadimitriou, K.D. *et al.*[106] have demonstrated a rational design method using molecular modeling (Figure S3(e)), for the liquid-phase exfoliation of graphene in a low-boiling point solvent, chloroform ($CHCl_3$). This was achieved using a unique architecture of pyrene end-capped poly(methyl methacrylate), PMMA, as the dispersing agent. Using Py-PMMA-Py as the stabilizer, they were able to achieve exfoliation of graphite in chloroform, towards a solution-phase synthesis of graphene sheets (with a control over the production of single-layer, few-layer, or multi-layer graphene), which can then be applied towards various applications.

The functionalization of graphene with small polycyclic aromatic hydrocarbons (PAHs) in organic solvents is a useful approach for controllably tuning the electronic properties of graphene. In very early work, Wang, X. *et al.*[107] used perylene tetracarboxylic acid (PTCA) to functionalize the graphene surface and selectively introduce densely packed surface groups on graphene. Using this, they were able to perform atomic layer deposition of metal oxide, Al_2O_3, on PTCA-coated graphene (Figure S3(f)). In further development, Wang, Q.H. and Hersam, M.C.[108] produced self-assembled monolayers of perylene-3,4,9,10-tetracarboxylic dianhydride (PTCDA) on epitaxial graphene grown on SiC substrate, with long-range molecular order in the form of a herringbone pattern (Figure S3(g)), unperturbed by defects in the underlying graphene or SiC substrate. Similarly, Kozhemyakina, N.V. *et al.*[109] have reported binding and electronic interaction of graphene with an organic dye molecule, perylene bisimide, in both thin film form and dispersed in homogeneous solution. These well-ordered structures can be used to generate self-assembled electronic and molecular sensors for detection applications, and are interesting from the point of view of the use of graphene in molecular electronics.

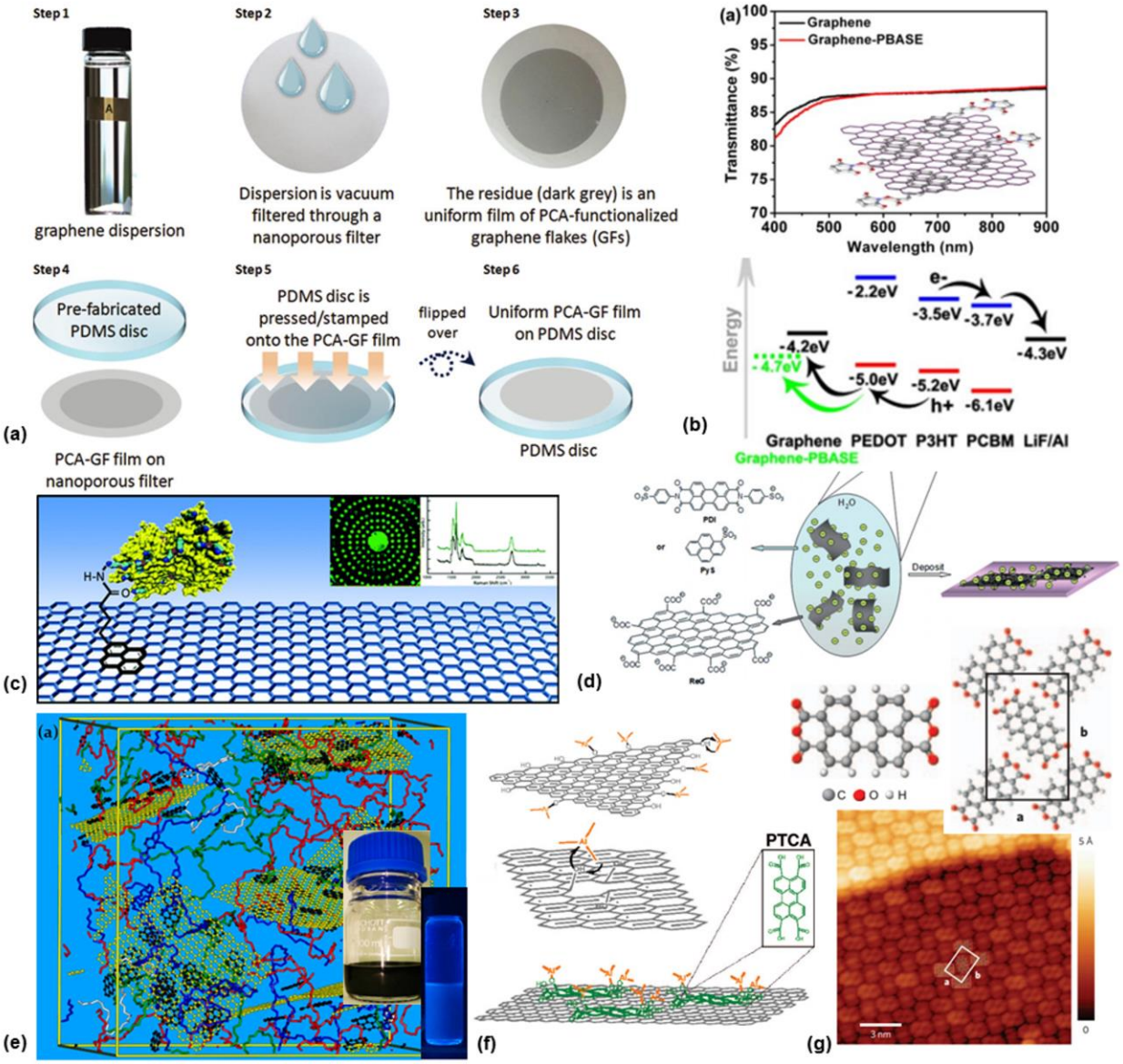

Figure S3: Non-covalent functionalization of graphene using pyrene derivatives.
(a) Flexible PCA-graphene-PDMS hybrid structures, with UV filtering. **(b)** High visible transmittance of graphene films with PBASE, with the energy diagram for a photovoltaic device. **(c)** Graphene coated with PYR-NHS, with inset showing micropatterning of proteins, glucose oxidase and laminin. **(d)** Electron-donor (PyS) and acceptor (PDI) aromatic molecules used to decorate graphene sheets. **(e)** MD simulations of Py-PMMA-Py adsorbed on graphene sheets. Inset shows the dispersion and blue photoluminescence of this functionalized graphene. **(f)** ALD of Al_2O_3 on PTCA-coated graphene. **(g)** Self-assembled monolayers of PTCDA, showing the molecular structure, herringbone unit cell, and molecular-resolution STM of the monolayer on the epitaxial graphene substrate. See text for definitions of molecules.
Reprinted (adapted) with permissions from: **(a, c, e, f)** An *et al.*[99], Kodali *et al.*[102], Papadimitriou *et al.*[106], Wang *et al.*[107] © 2011, 2011, 2016, 2008 American Chemical Society respectively. **(b)** Wang *et al.*[101] © 2009 AIP Publishing. **(d)** Su *et al.*[104] © 2009 John Wiley and Sons. **(g)** Wang and Hersam[108] © 2009 Nature Publishing Group.

5.2 Porphyrin and its derivatives

Porphyrins have been widely deployed for the functionalization of carbon nanotubes, due to their π-π interactions, for use in applications such as sunlight harvesting. Similarly, there have been investigations into the use of porphyrins for exfoliating graphene. A metalloporphyrin derivative, 5,10,15,20-*tetrakis*[$\alpha\alpha\alpha\alpha$-2-trismethyl-ammoniomethylphenyl] porphyrin iron (III) pentachloride (FeTMAPP), also known as picket-fence iron porphyrin, was used by Tu, W. *et al.*[110] to synthesize a water-soluble nanocomposite of rGO, with good dispersion in a stable and homogeneous suspension. Upon implementation in an electrode for a redox couple, the device showed very good electrochemical performance for highly sensitive amperometric biosensing of the chlorite molecule (Figure 6(f) in the Main Text), due to the synergistic effect between the rGO and the porphyrin. At around the same time, Geng, J. and Jung, H-T.[111] reported a technique for using porphyrin to functionalize chemically-derived graphene from hydrazine-reduced GO. The resulting graphene had a low sheet resistance ~ 5 kΩ/□, with > 80% optical transparency at λ = 550 nm. More recently, Zhang, S. *et al.*[112] have proposed the development of a biosensor for the detection of glucose in human serum. This was achieved by functionalizing electrodes composed of reduced graphene nanoribbons with iron(III) *meso-tetrakis*(N-methyl pyridinium-4-yl)-porphyrin (FeTMPyP), which showed enhanced electrocatalytic activity towards the reduction of dissolved oxygen catalyzed by the enzyme glucose oxidase (Figure 6(g) in the Main Text), and the detection of glucose is based on this redox reaction.

5.3 Halogenation and Hydrogenation

It is possible to attach atoms or other functional groups to the sp^2 carbon atoms in the graphene basal plane. If hydrogen is used, for example, the resulting material, "graphane", is completely saturated[113] to sp^3, while maintaining the 2D structure and hexagonal symmetry of graphene. A consequence of this transition is that the charge carrier mobility is smaller by about ~ 2-3 orders-of-magnitude, behaving as an insulator, with a band gap of ~ 3.5 eV at the Γ-point. Shortly after the theoretical hypothesis of its existence, graphane was synthesized by Elias, D.C. *et al.*[114], through the reversible hydrogenation of single-layer graphene. A low-pressure (0.1 mbar) dc plasma treatment in H_2(10%)-Ar mixture for 2 hr. results in saturated graphane, while annealing the material at 450 °C for 24hr. results in de-hydrogenation back to graphene. Alternatively, Ryu, S. *et al.*[115] have developed a method for *in situ* hydrogenation (reversible) of graphene by the electron-induced dissociation of hydrogen silsesquioxane (HSQ). While it has been proposed that graphane can find suitable applications in various fields such as hydrogen storage, thermoelectrics, piezo

electricity, frictionless surfaces etc., owing to its unique structure and electronic properties[116], applications in the biomedical sector are few, till date. In one example, Tan, S.M. *et al.*[117] have performed a comparative analysis of graphane with ordinary graphene for the electrochemical oxidation performance of biomarker molecules such as ascorbic acid, dopamine and uric acid, which could have potential applications in biosensing devices.

Similar to graphane, fluorographene or graphene fluoride can also be synthesized, by the fluorination of graphene by exposure to XeF_2 at elevated[118] (70 - 200 °C), or at room temperature[119]. Graphene fluoride has also been synthesized in the literature from graphite fluoride by mechanical exfoliation, in a manner analogous to the "scotch-tape" method used for the first synthesis of graphene. Graphene fluoride is an insulator, with resistivity > 10^{12} Ω. As the 2D analog of Teflon (poly tetrafluoroethylene), fluorographene is thermally stable at temperatures up to 400 °C, with further heating resulting in defluorination with the evolution of compounds such as CF_4, C_2F_4, C_2F_6 etc. Density functional theory (DFT) calculations suggest[120] that the stability of other graphene halides (C_1X_1) decreases in the order X = F > Cl > Br > I, with fluorographene even more chemically stable than graphane[121]. However, it has been shown that it is possible to synthesize "chemically-derived graphene" from reduced graphene fluoride[122], analogous to preparing rGO from GO[123].

5.4 Nucleophilic Addition Reactions on graphene

1,3-dipolar cycloaddition of azomethine ylides (the Prato reaction) has also been used to functionalize graphene, analogous to the method described for SWNTs in Section 3.2.1. as a result of this reaction, the graphene sheets are decorated with dihydroxyl phenyl groups, by pyrrolidine rings which form perpendicular (out-of-plane) to the basal plane by the addition of azomethine ylide precursors. Because of the flexibility of this reaction, it is possible to introduce different functional groups. For example, Quintana, M. *et al.*[124] have used this cycloaddition reaction to attach amino-functional groups to the graphene sheet, followed subsequently by selective binding of gold nanorods to the graphene reactive sites. It was shown that the reaction takes place not only at the edges of the graphene sheet, but uniformly distributed all over the basal plane, including the internal C=C bonds of graphene. Alternatively, Liu, L-H. *et al.*[125] have derivatized graphene with different functional groups, by treating solvent-exfoliated graphene with perfluorophenyl azide (PFPA), through photochemical or thermal activation. Nitrene chemistry has also been used as a general approach to produce solubilized graphene nanosheets, by several researchers, such as Choi, J. *et al.*[126], He, H. *et al.*[127], and Zhong, X. *et al.*[128]

Table 3: A summary of the comparison of functionalization schemes for graphene and its derivatives.
The metrics used for the comparison are described in the text in Section 2 above.
Phases: S (solid), L (liquid), G (gas), TF (thin film), aq. (aqueous medium)
Characterization techniques: SEM/TEM: Scanning / Transmission electron microscopy, PL: photoluminescence, UV-vis: Ultraviolet / visible absorbance spectroscopy, TGA: thermogravimetry analysis, XPS: X-ray photoelectron spectroscopy, NMR: nuclear magnetic resonance, AFM: atomic force microscopy, FTIR: Fourier Transform infrared spectroscopy, ICP-AES: inductively coupled plasma atomic emission spectroscopy

Agent of Functionalization	# of Steps (Time reqd.)	Special Equipment?	Phase of Func.	Properties affected (+/–)	Characterization Techniques	Scalable?	Reproducible?	Applications
Non-covalent Functionalization								
(1) Aromatic molecules								
Pyrene and its derivatives (PCA, PBASE, 1-pyrenebutyrate, PTCA, PTCDA, 1-nitropyrene, perylene bisimide, perylene diimide	1 (up to 24 hr.)	Membrane (PDMS, cellulose) filtration, ultrahigh vac. CVD	L (aq.), S, TF	Dispersion in water (++), Fluorescence quenching (—)	UV-vis, STM, AFM, XRD, FTIR, Raman, XPS, UPS	High	General	UV protection[99], hole doping (increased inter-layer conductivity)[100], improved efficiency of PV devices[101], micro-patterning proteins/enzymes for monitoring glucose, cells, tissue engineering[102], self-assembled molecules (long-range order)[108]
Porphyrin and its derivatives (FeTMAPP, FeTMPyP)	1 (10 min. - 1 hr.)	No	L (aq.), TF	Light harvesting (+++), Fluorescence quenching (–)	AFM, TEM, Raman, UV-vis, Cyclic voltammetry	High	General	Sunlight harvesting, optical transparency[111], amperometric biosensing of chlorite for drinking water disinfection[110], blood glucose detection[112]
(2) Polymer adsorption								
DNA-based composites	1 (2 - 54 hr.)	Low-T drying oven	L (aq.)	High adsorption capability (+++), High binding affinity (+/–), Fluorescence quenching (++)	SEM, AFM, XPS, Fluorometer	Low	General[129]	DNA Origami[130], single-bacterial cell detection, label-free DNA sensing[131], patterning of nanoparticles[132], biomolecule detection[133], 3D self-healing hydrogels[134] with high dye-loading, DNA sequencing[135]
Poly (ethylene glycol), PEG, and derivatives like PL–PEG–NH_2	1 (72 hr.)	γ-irradiation chamber	L (aq.), TF	Dispersion (+++), selectivity to binding agents (++), improved lubrication, decreased friction resistance (+++)	SEM, HRTEM, XPS, FTIR, UV-vis	High	General[136]	Photoablation of cells[137], capture of CTCs from whole blood[138,139], solid-state lubrication[140]
(3) Other Approaches								
Mild Thermal Annealing	1 (1 - 9 days)	No	L (aq.), TF, S	Conductivity (+++), Absorbance (++), PL blue-shift (++)	Nano-Auger, 2D Raman, XPS, 4-point probe	High	General[141,142]	Enhance the density of functionalization of antibodies grafted on GO

Agent of Functionalization	# of Steps (Time reqd.)	Special Equipment?	Phase of Func.	Properties affected (+/–)	Characterization Techniques	Scalable?	Reproducible?	Applications
Covalent Functionalization								
(1) Direct Chemical Reactions								
Halogenation (with XeF_2, or exfoliation from graphene fluoride) and Hydrogenation (with H_2, HSQ)	1 (5 min.- 2 hr.)	Glove box (atm/moisture control), low-pressure dc plasma	S, TF	Optical bandgap (++), high-temperature stability (++), High mechanical strength and elasticity (+++), High resistivity (+/–)	XPS, Raman, SAED, UV-vis, *I-V* curves	High	General	Electrochemical oxidation of ascorbic acid, dopamine, uric acid for biosensing[117], hydrogen storage, thermoelectric materials, electronic insulator (2D analog of Teflon) with resistivity > 10^{12} Ω
Radical addition (diazo coupling, reactions with azomethine ylides, photochemical addition of benzoyl peroxides, nitrenes, sulfonation with sulfanilic acid)	1 (2 - 7 days)	Sonicator, ice bath, N_2 ambient, vac. drying	L	Stability in physiological media (+++), mixed loading capability, pH-responsive (+), fluorescence / phosphorescence quenching (+/–)	FTIR, UV-vis, AFM, TEM, Phosphorescence lifetime, TGA, Raman	High	General[143]	Introducing band gap (~ 0.4 eV) in graphene[144], effective binding of Au nanorods[124], synergistic loading of 2 anticancer drugs[145], folate-targeted delivery and enhanced chemo-therapeutic efficacy by apoptotic cell-cycle arrest[146], multifunctional graphene with magnetic and fluorescence[147]
(2) Polymer conjugation								
Poly (ethylene glycol), PEG and other polymers like poly (L-lysine) PLL, poly (vinyl alcohol), PVA, polystyrene PS, poly (vinylpyrrolidone) PVP	1-2, (5 min. - 24 hr., depending on polymer)	Sonicator	L	High physiological stability (+++), high loading capacity (++)	AFM, FTIR, UV-vis	High	General	Load and deliver water-insoluble anti-cancer drugs[148], EPR targeting of tumors[149], NIR photothermal therapy[150], photodynamic therapy enhanced with PTT[151], diffusion-weighted MRI[152], light-controlled delivery of siRNA[153], biosensing of H_2O_2[154], PET imaging of xenograft tumors through active vascular targeting[155]
EDC "click" chemistry	3 (48 hr.)	No	TF	Binding affinity (+++), Specificity (++), Fluorescence (+++)	AFM, Confocal Microscopy	High	Self	Capture of white blood cells from whole blood[156]

6. Safety and Toxicity Aspects of CANOMATs for Biomedical Applications

A Review of the advances in functionalization of CANOMATs for biomedical applications would not be meaningfully complete without a brief overview of the safety and toxicity aspects of these materials. This is important because any potential commercial application towards the use of CANOMATs for human diagnostics or treatment would have to pass the scrutiny of the Food and Drug Administration (FDA) in the United States (and the corresponding regulatory bodies elsewhere in the world), for which they have to demonstrate safety at the intended dosage of application (in addition to establishing efficacy). The toxicity of carbon nanomaterials depends on the degree of agglomeration when used in *in vitro* or *in vivo* applications. This can be modified to a great extent by the choice and density[157] of functionalization agent, the dosage[158] used, and the size[159] of the nanomaterial.

In one of the fist comparative studies of the *in vitro* cytotoxicity, Jia, G. *et al.*[160] have compared the relative cytotoxicity of C_{60}, SWNTs, and multi-walled carbon nanotubes (Figure S4(a)) to alveolar macrophages. Through an MTT assay, they reported signs of apoptotic cell death, with a toxicity in the order of SWNTs > MWNT (10 - 20 nm) > C_{60}, with quite different toxic dosages ~ 0.38, 3.06 and 226.0 $\mu g/cm^2$ at 6 hr. exposures, respectively. However, the limitation of such an assay is that bioactivity and toxicity in the complex *in vivo* microenvironment may differ significantly from such a cell assay. In a separate study, Manna, S.K. *et al.*[161] have investigated the cause of toxicity of SWNTs, in an assessment in human keratinocyte cells. They concluded that increased oxidative stress caused by SWNT dosing, leading to downstream activation of the NF-κB nuclear transcription factor, results in cell death by apoptosis or necrosis. In a study of the effect of functionalization on cellular trafficking, Kostarelos, K. *et al.*[162] reported that functionalized carbon nanotubes are capable of being taken up by both mammalian and prokaryotic cells, and penetrating the various intracellular barriers by energy-independent mechanisms, which is aided by their high aspect ratio, analogous to a "nanosyringe effect" (Figure S4(c)). Several other groups of researchers, such as Hu, X. *et al.*[163], Arora, S. *et al.*[164] and Breznan, D. *et al.*[165] have studied the interaction of carbon nanotubes with human and murine cell lines, and the studies basically converge to the same conclusion, i.e. the toxicity is dosage-dependent, and it can be mitigated to a large extent by effective functionalization. For example, Cherukuri, P. *et al.*[166] incubated cultured macrophages with a suspension of SWNTs in Pluronic surfactant. The nanotubes were reported to be actively ingested, with no observable detrimental effect on the cell viability (Figure S4(b)), up to concentrations of ~ 4 μg/ml with exposures up to 96 hr. Similarly, Hong, G.S. *et al.*[78] have demonstrated that PEG-coated SWNTs show a very high IC_{50} value (the half-maximal inhibitory concentration), ~ 150 - 200 μg/ml (Figure S4(h)). In a similar vein, two-dimensional CANOMATs, including graphene and its derivatives, are considered to be less cytotoxic, when functionalized, such as GO. As is the case with SWNTs, pristine graphene is believed to trigger two signaling pathways: the MAPK (nitrogen-activated protein kinase) and the TGF-β (transforming growth factor beta), both of which lead to apoptotic cell death. GO has been proposed to be an excellent material for biological applications[167], owing to its intrinsic fluorescence, excellent water solubility without the need for surfactants, absence of metallic impurities (unlike carbon nanotubes) causing oxidative stresses, and its high surface area, which allows for loading of drugs and other molecules. Liao, K.H. *et al.*[168] have reported the first study of the blood compatibility of graphene and GO on human RBCs and skin fibroblast cells, in which they investigated the hemolytic activity of GO and graphene sheets

of various sizes (Figure S4(d)). Treatment with chitosan was reported to eliminate the hemolytic activity; thereby highlighting the importance of functionalization. At high concentration ~ 50 μg/ml, it has been shown that GO does cause slight reduction in the cell viability[169], owing to dose-dependent oxidative stress, although, overall, GO is considered to be a safe material at the cellular level. In an alternative approach, Hu, W. *et al.*[170] have demonstrated that the adsorption of proteins, such as fetal bovine serum (FBS, 10%, typically present in culture media) can greatly mitigate the concentration-dependent cytotoxicity of GO, by minimizing the physical damage to the cell membrane caused by direct interaction with the GO nanosheets. Several groups of researchers have effectively used PEGylation as a means to reduce the cytotoxicity of GO. For example, Liu, Z. *et al.*[148] and Sun, X. *et al.*[171] have developed PEGylated nanographene oxide (NGO-PEG) as a highly potent nanocarrier complex for the delivery of a water-insoluble chemotherapeutic drug, as well as for live cell imaging in the near-infrared, by non-covalent van der Waals interaction with the GO.

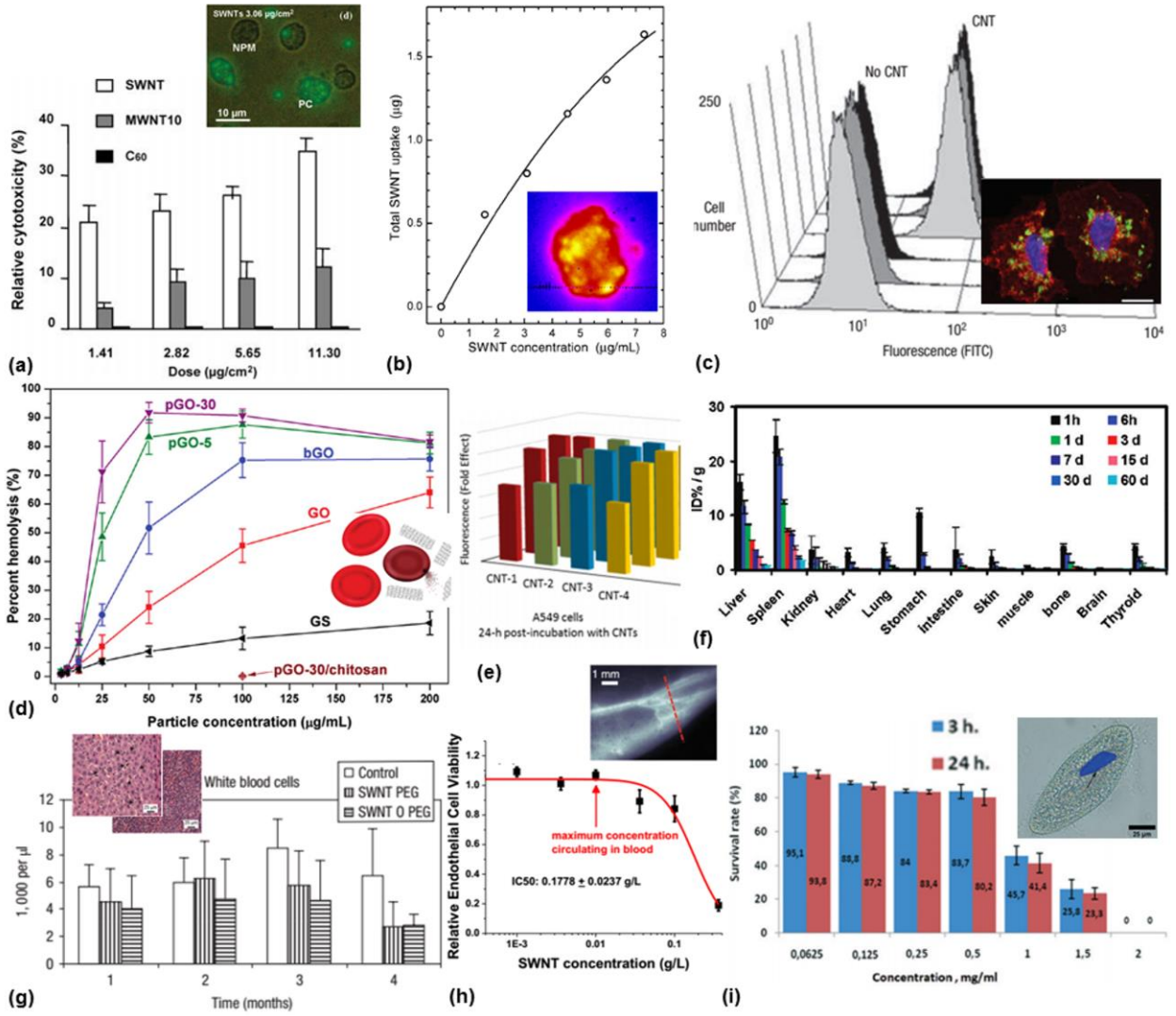

Figure S4: *In vitro* and *in vivo* cytotoxicity of CANOMATs.

(a) Relative toxicity of fullerenes, single- and multi-walled carbon nanotubes to alveolar macrophages. Inset shows cells becoming non-phagocytic after exposure to CANOMATs. **(b)** Amount of internalized SWNT in macrophages increases with the exposure concentration. Inset: NIR fluorescence image, showing localization in vesicles. **(c)** "Nanosyringe effect": Cellular trafficking of functionalized CNTs continues even under endocytosis-inhibiting conditions (grey-to-black, increasing conc. of NaN_3). Inset: confocal image, showing CNT (green) localization in the perinuclear region (blue). **(d)** Hemolysis of human RBCs upon incubation with non-functionalized GO and rGO. Toxicity depends on degree of aggregation. **(e)** CANOMATs can quench the optical readouts for *in vitro* assays, potentially skewing cytotoxicity measurements. **(f)** Long-term (60-day) study of the biodistribution of PEG-functionalized nano graphene, indicating RES uptake. **(g)** Toxicology study of SWNTs in mice. Blood chemistries (shown here: WBC populations) did not vary significantly between control and PEG-SWNT treated groups. Inset: SWNT-PEG observed in liver and spleen cells (black arrows), without signs of tissue damage. **(h)** IC_{50} ~ 0.18 mg/ml for DSPE-mPEG-SWNT, ~ 17× lower than the typical dosage. Inset shows example of imaging hind leg blood vessels using functionalized SWNTs. **(i)** Acute toxicity of GO nanoflakes at ≥ 1 mg/ml, in a protozoan organism. Inset shows deformity in nucleus (blue) after exposure. See text for definitions of molecules.
Reprinted (adapted) with permissions from: **(a, b, d, f)** Jia *et al.*[160], Cherukuri *et al.*[166], Liao *et al.*[168], Yang *et al.*[172] © 2005, 2004, 2011, 2011 American Chemical Society respectively. **(e)** Breznan *et al.*[165] © 2015 Elsevier Publishing Group. **(c, g, h)** Kostarelos *et al.*[162], Schipper *et al.*[173], Hong *et al.*[78] © 2007, 2008, 2012 Nature Publishing Group respectively. **(i)** Kryuchkova *et al.*[174] © 2016 Royal Society of Chemistry.

The jury is still out[175] on the *in vivo* circulation, pharmacokinetics, biodistribution and toxicity of CANOMATs, and much work remains to be done in order to ascertain safe doses of these materials for biomedical applications. Independently, Singh, R. *et al.*[176] reported that diethylentriaminepentaacetic acid (DTPA)-functionalized SWNT showed rapid renal clearance from systemic blood circulation after i.v. injection, with a half-life ~ 3 hr. In one of the first pilot studies of the long-term toxicology of SWNTs, Schipper, M.L. *et al.*[173] examined the acute and chronic toxicity of functionalized SWNTs (Figure S4(g)) when injected into the bloodstream of healthy mice. It was reported that the carbon nanotubes persisted within the macrophages of the liver and the spleen for 4 months (the duration of the study), without apparent toxicity. Similarly, Liu, Z. *et al.*[177] have measured the blood circulation of i.v.-injected SWNTs, and monitored their distribution over a period of 3 months, using Raman spectroscopy. They reported that PEG-functionalized SWNTs offer the longest blood circulation lifetime, ~ 1 day, with relatively low uptake in the RES system, and almost complete clearance from the main organs in the body within ~ 2 months post injection. The circulation kinetics and uptake of the nanomaterial in the various organs can be tuned, to a certain extent, by the length of the PEG chain, and by its architecture (linear or branched)[178]. Moving further, for 2D CANOMATs, recent work by Liu, Y. *et al.*[179] suggests that bare GO can induce mutagenesis both *in vitro* (at concentrations of 10 and 100 μg/ml) and *in vivo* (injected at a dose of 4 mg/kg for 5 consecutive days), and thereby extra surface modification is deemed to be necessary for the use of GO in biomedical applications. This is surprising – considering that several groups of researchers had considered GO to be an overall "safe" material at the cellular level, as discussed in the previous paragraph. Even before these results were known, Zhang, S. *et al.*[180] have shown that functionalization with dextran, another biocompatible polymer widely used for the coating of biomaterials, offers remarkable reduction in short-term toxicity, with rapid clearance from the RES system in mice. Similarly, Yang, K. *et al.*[172] have studied the long-term biodistribution and toxicology of PEGylated graphene in mice. Although these materials accumulate in the liver and

spleen, they are gradually cleared by renal and fecal excretion pathways (Figure S4(f)), and there was no observed toxicity at a significantly high dose (20 mg/kg) over a period of 3 months. The same group of researchers reported[181] no uptake in tissues after oral administration indicating very little intestinal absorption of PEGylated GO, but high accumulation in the liver and spleen after intraperitoneal (i.p.) injection, due to engulfment by phagocytes. In another approach to functionalization, Singh, S.K. *et al*.[182] have developed amine-modified graphene (G–NH_2), which, upon i.v. administration, showed no stimulatory effects on human platelets or evoke lysis of erythrocytes, nor did it induce pulmonary thromboembolism, compared to bare unmodified GO or rGO. As an interesting aside from mammalian studies, a recent study[174] comparing the toxicity of various clays, silica nanomaterials and GO in a model protozoan organism (*Paramecium caudatum*) found complete inhibition of fertility by GO, with sizable toxic effects becoming apparent at dosages as low as 100 μg/ml (Figure S4(i)). For a comprehensive review on the *in vitro* and *in vivo* toxicity of fullerene and carbon nanotube derivatives, the reader is referred to Lalwani, G. *et al.*[183], and Harrison, B.S. and Atala, A.[184] respectively, and to Seabra, A.B. *et al*.[185] for graphene and its derivatives, which is beyond the scope of the current discussion on functionalization techniques.

References

1. H. W. Kroto, J. R. Heath, S. C. O'Brien, R. F. Curl, and R. E. Smalley: C60: Buckminsterfullerene. *Nature* **318**(6042), 162 (1985).
2. M. Arndt, O. Nairz, J. Vos-Andreae, C. Keller, G. van der Zouw, and A. Zeilinger: Wave–particle duality of C60 molecules. *Nature* **401**(6754), 680 (1999).
3. A. K. Geim and K. S. Novoselov: The rise of graphene. *Nat. Mater.* **6**(3), 183 (2007).
4. M. S. Dresselhaus, G. Dresselhaus, and P. Avouris: Carbon Nanotubes: Synthesis, Structure, Properties, and Applications (Springer, 2001).
5. S. M. Bachilo, M. S. Strano, C. Kittrell, R. H. Hauge, R. E. Smalley, and R. B. Weisman: Structure-Assigned Optical Spectra of Single-Walled Carbon Nanotubes. *Science* **298**(5602), 2361 (2002).
6. R. Saito, M. Fujita, G. Dresselhaus, and M. S. Dresselhaus: Electronic structure of chiral graphene tubules. *Appl. Phys. Lett.* **60**(18), 2204 (1992).
7. K. Kato, T. Koretsune, and S. Saito: Energetics and electronic properties of twisted single-walled carbon nanotubes. *Phys. Rev. B* **85**(11), 115448 (2012).
8. S. Iijima, C. Brabec, A. Maiti, and J. Bernholc: Structural flexibility of carbon nanotubes. *J. Chem. Phys.* **104**(5), 2089 (1996).
9. E. W. Wong, P. E. Sheehan, and C. M. Lieber: Nanobeam Mechanics: Elasticity, Strength, and Toughness of Nanorods and Nanotubes. *Science* **277**(5334), 1971 (1997).
10. S. R. Mehrotra and G. Klimeck: (2010).
11. K. Nakada, M. Fujita, G. Dresselhaus, and M. S. Dresselhaus: Edge state in graphene ribbons: Nanometer size effect and edge shape dependence. *Phys. Rev. B* **54**(24), 17954 (1996).
12. X. Du, I. Skachko, A. Barker, and E. Y. Andrei: Approaching ballistic transport in suspended graphene. *Nat. Nanotechnol.* **3**(8), 491 (2008).
13. A. A. Balandin: Thermal properties of graphene and nanostructured carbon materials. *Nat. Mater.* **10**(8), 569 (2011).
14. K. S. Novoselov, A. K. Geim, S. V. Morozov, D. Jiang, Y. Zhang, S. V. Dubonos, I. V. Grigorieva, and A. A. Firsov: Electric Field Effect in Atomically Thin Carbon Films. *Science* **306**(5696), 666 (2004).
15. B. Chase, N. Herron, and E. Holler: Vibrational spectroscopy of fullerenes (C60 and C70). Temperature dependant studies. *J. Phys. Chem.* **96**(11), 4262 (1992).
16. M. S. Dresselhaus, A. Jorio, M. Hofmann, G. Dresselhaus, and R. Saito: Perspectives on Carbon Nanotubes and Graphene Raman Spectroscopy. *Nano Lett.* **10**(3), 751 (2010).
17. M. S. Dresselhaus, G. Dresselhaus, and P. C. Eklund: Raman Scattering in Fullerenes. *J. Raman Spectrosc.* **27**(3–4), 351 (1996).
18. J. Menéndez and J. B. Page: in *Light Scatt. Solids VIII* (Springer, 2000), pp. 27–95.
19. H. Kuzmany, R. Pfeiffer, M. Hulman, and C. Kramberger: Raman spectroscopy of fullerenes and fullerene–nanotube composites. *Philos. Trans. R. Soc. Lond. Math. Phys. Eng. Sci.* **362**(1824), 2375 (2004).

20. A. C. Ferrari and J. Robertson: Interpretation of Raman spectra of disordered and amorphous carbon. *Phys. Rev. B* **61**(20), 14095 (2000).
21. C. Branca, F. Frusteri, V. Magazù, and A. Mangione: Characterization of Carbon Nanotubes by TEM and Infrared Spectroscopy. *J. Phys. Chem. B* **108**(11), 3469 (2004).
22. M. Prato: [60]Fullerene chemistry for materials science applications. *J. Mater. Chem.* **7**(7), 1097 (1997).
23. K. Komatsu, M. Murata, and Y. Murata: Encapsulation of Molecular Hydrogen in Fullerene C60 by Organic Synthesis. *Science* **307**(5707), 238 (2005).
24. D. M. Guldi: Fullerene – porphyrin architectures; photosynthetic antenna and reaction center models. *Chem. Soc. Rev.* **31**(1), 22 (2002).
25. H. Imahori: Porphyrin–fullerene linked systems as artificial photosynthetic mimics. *Org. Biomol. Chem.* **2**(10), 1425 (2004).
26. G. Li, R. Zhu, and Y. Yang: Polymer solar cells. *Nat. Photonics* **6**(3), 153 (2012).
27. F. Li, K. G. Yager, N. M. Dawson, Y.-B. Jiang, K. J. Malloy, and Y. Qin: Stable and Controllable Polymer/Fullerene Composite Nanofibers through Cooperative Noncovalent Interactions for Organic Photovoltaics. *Chem. Mater.* **26**(12), 3747 (2014).
28. G. Yu, J. Gao, J. C. Hummelen, F. Wudl, and A. J. Heeger: Polymer Photovoltaic Cells: Enhanced Efficiencies via a Network of Internal Donor-Acceptor Heterojunctions. *Science* **270**(5243), 1789 (1995).
29. F. Diederich and C. Thilgen: Covalent Fullerene Chemistry. *Science* **271**(5247), 317 (1996).
30. A. Bianco, M. Maggini, G. Scorrano, C. Toniolo, G. Marconi, C. Villani, and M. Prato: Synthesis, Chiroptical Properties, and Configurational Assignment of Fulleroproline Derivatives and Peptides. *J. Am. Chem. Soc.* **118**(17), 4072 (1996).
31. S. Bosi, T. Da Ros, G. Spalluto, and M. Prato: Fullerene derivatives: an attractive tool for biological applications. *Eur. J. Med. Chem.* **38**(11–12), 913 (2003).
32. M. Carravetta, A. Danquigny, S. Mamone, F. Cuda, O. G. Johannessen, I. Heinmaa, K. Panesar, R. Stern, M. C. Grossel, A. J. Horsewill, A. Samoson, M. Murata, Y. Murata, K. Komatsu, and M. H. Levitt: Solid-state NMR of endohedral hydrogen–fullerene complexes. *Phys. Chem. Chem. Phys.* **9**(35), 4879 (2007).
33. W.-B. Ko and K.-N. Baek: The oxidation of fullerenes (C60, C70) with various oxidants under ultrasonication. *Phys. Solid State* **44**(3), 424 (2002).
34. P. Chaudhuri, A. Paraskar, S. Soni, R. A. Mashelkar, and S. Sengupta: Fullerenol−Cytotoxic Conjugates for Cancer Chemotherapy. *ACS Nano* **3**(9), 2505 (2009).
35. R. Injac, M. Perse, M. Cerne, N. Potocnik, N. Radic, B. Govedarica, A. Djordjevic, A. Cerar, and B. Strukelj: Protective effects of fullerenol C60(OH)24 against doxorubicin-induced cardiotoxicity and hepatotoxicity in rats with colorectal cancer. *Biomaterials* **30**(6), 1184 (2009).
36. R. Partha, L. R. Mitchell, J. L. Lyon, P. P. Joshi, and J. L. Conyers: Buckysomes: Fullerene-Based Nanocarriers for Hydrophobic Molecule Delivery. *ACS Nano* **2**(9), 1950 (2008).
37. E. Nakamura, H. Isobe, N. Tomita, M. Sawamura, S. Jinno, and H. Okayama: Functionalized Fullerene as an Artificial Vector for Transfection. *Angew. Chem. Int. Ed.* **39**(23), 4254 (2000).

38. R. Maeda-Mamiya, E. Noiri, H. Isobe, W. Nakanishi, K. Okamoto, K. Doi, T. Sugaya, T. Izumi, T. Homma, and E. Nakamura: In vivo gene delivery by cationic tetraamino fullerene. *Proc. Natl. Acad. Sci.* **107**(12), 5339 (2010).
39. S. Aime, M. Botta, and E. Terreno: in *Adv. Inorg. Chem.*, edited by B.-A. in I. Chemistry (Academic Press, 2005), pp. 173–237.
40. M. Mikawa, H. Kato, M. Okumura, M. Narazaki, Y. Kanazawa, N. Miwa, and H. Shinohara: Paramagnetic Water-Soluble Metallofullerenes Having the Highest Relaxivity for MRI Contrast Agents. *Bioconjug. Chem.* **12**(4), 510 (2001).
41. P. P. Fatouros, F. D. Corwin, Z.-J. Chen, W. C. Broaddus, J. L. Tatum, B. Kettenmann, Z. Ge, H. W. Gibson, J. L. Russ, A. P. Leonard, J. C. Duchamp, and H. C. Dorn: In Vitro and in Vivo Imaging Studies of a New Endohedral Metallofullerene Nanoparticle. *Radiology* **240**(3), 756 (2006).
42. R. D. Bolskar, A. F. Benedetto, L. O. Husebo, R. E. Price, E. F. Jackson, S. Wallace, L. J. Wilson, and J. M. Alford: First Soluble M@C60 Derivatives Provide Enhanced Access to Metallofullerenes and Permit in Vivo Evaluation of Gd@C60[C(COOH)2]10 as a MRI Contrast Agent. *J. Am. Chem. Soc.* **125**(18), 5471 (2003).
43. P. Mroz, G. P. Tegos, H. Gali, T. Wharton, T. Sarna, and M. R. Hamblin: Photodynamic therapy with fullerenes. *Photochem. Photobiol. Sci.* **6**(11), 1139 (2007).
44. J. Liu, S. Ohta, A. Sonoda, M. Yamada, M. Yamamoto, N. Nitta, K. Murata, and Y. Tabata: Preparation of PEG-conjugated fullerene containing Gd3+ ions for photodynamic therapy. *J. Controlled Release* **117**(1), 104 (2007).
45. J. Chen, M. A. Hamon, H. Hu, Y. Chen, A. M. Rao, P. C. Eklund, and R. C. Haddon: Solution Properties of Single-Walled Carbon Nanotubes. *Science* **282**(5386), 95 (1998).
46. K. Kamaras, M. E. Itkis, H. Hu, B. Zhao, and R. C. Haddon: Covalent Bond Formation to a Carbon Nanotube Metal. *Science* **301**(5639), 1501 (2003).
47. V. Georgakilas, K. Kordatos, M. Prato, D. M. Guldi, M. Holzinger, and A. Hirsch: Organic Functionalization of Carbon Nanotubes. *J. Am. Chem. Soc.* **124**(5), 760 (2002).
48. N. Tagmatarchis and M. Prato: Functionalization of carbon nanotubes via 1,3-dipolar cycloadditions. *J. Mater. Chem.* **14**(4), 437 (2004).
49. M. Holzinger, O. Vostrowsky, A. Hirsch, F. Hennrich, M. Kappes, R. Weiss, and F. Jellen: Sidewall Functionalization of Carbon Nanotubes. *Angew. Chem. Int. Ed.* **40**(21), 4002 (2001).
50. Z. Yinghuai, A. T. Peng, K. Carpenter, J. A. Maguire, N. S. Hosmane, and M. Takagaki: Substituted Carborane-Appended Water-Soluble Single-Wall Carbon Nanotubes: New Approach to Boron Neutron Capture Therapy Drug Delivery. *J. Am. Chem. Soc.* **127**(27), 9875 (2005).
51. H. Dumortier, S. Lacotte, G. Pastorin, R. Marega, W. Wu, D. Bonifazi, J.-P. Briand, M. Prato, S. Muller, and A. Bianco: Functionalized Carbon Nanotubes Are Non-Cytotoxic and Preserve the Functionality of Primary Immune Cells. *Nano Lett.* **6**(7), 1522 (2006).
52. A. Hamwi, H. Alvergnat, S. Bonnamy, and F. Béguin: Fluorination of carbon nanotubes. *Carbon* **35**(6), 723 (1997).
53. E. T. Mickelson, C. B. Huffman, A. G. Rinzler, R. E. Smalley, R. H. Hauge, and J. L. Margrave: Fluorination of single-wall carbon nanotubes. *Chem. Phys. Lett.* **296**(1–2), 188 (1998).

54. K. N. Kudin, H. F. Bettinger, and G. E. Scuseria: Fluorinated single-wall carbon nanotubes. *Phys. Rev. B* **63**(4), 45413 (2001).
55. Z. Gu, H. Peng, R. H. Hauge, R. E. Smalley, and J. L. Margrave: Cutting Single-Wall Carbon Nanotubes through Fluorination. *Nano Lett.* **2**(9), 1009 (2002).
56. P. E. Pehrsson, W. Zhao, J. W. Baldwin, C. Song, J. Liu, S. Kooi, and B. Zheng: Thermal Fluorination and Annealing of Single-Wall Carbon Nanotubes. *J. Phys. Chem. B* **107**(24), 5690 (2003).
57. R. Barthos, D. Méhn, A. Demortier, N. Pierard, Y. Morciaux, G. Demortier, A. Fonseca, and J. B. Nagy: Functionalization of single-walled carbon nanotubes by using alkyl-halides. *Carbon* **43**(2), 321 (2005).
58. V. K. Abdelkader, S. Scelfo, C. García-Gallarín, M. L. Godino-Salido, M. Domingo-García, F. J. López-Garzón, and M. Pérez-Mendoza: Carbon Tetrachloride Cold Plasma for Extensive Chlorination of Carbon Nanotubes. *J. Phys. Chem. C* **117**(32), 16677 (2013).
59. J.-F. Colomer, R. Marega, H. Traboulsi, M. Meneghetti, G. Van Tendeloo, and D. Bonifazi: Microwave-Assisted Bromination of Double-Walled Carbon Nanotubes. *Chem. Mater.* **21**(20), 4747 (2009).
60. Y. A. Mackeyev, J. W. Marks, M. G. Rosenblum, and L. J. Wilson: Stable Containment of Radionuclides on the Nanoscale by Cut Single-Wall Carbon Nanotubes. *J. Phys. Chem. B* **109**(12), 5482 (2005).
61. Y. Chen, R. C. Haddon, S. Fang, A. M. Rao, P. C. Eklund, W. H. Lee, E. C. Dickey, E. A. Grulke, J. C. Pendergrass, A. Chavan, B. E. Haley, and R. E. Smalley: Chemical Attachment of Organic Functional Groups to Single-walled Carbon Nanotube Material. *J. Mater. Res.* **13**(9), 2423 (1998).
62. S. Pekker, J.-P. Salvetat, E. Jakab, J.-M. Bonard, and L. Forró: Hydrogenation of Carbon Nanotubes and Graphite in Liquid Ammonia. *J. Phys. Chem. B* **105**(33), 7938 (2001).
63. A. Nikitin, H. Ogasawara, D. Mann, R. Denecke, Z. Zhang, H. Dai, K. Cho, and A. Nilsson: Hydrogenation of Single-Walled Carbon Nanotubes. *Phys. Rev. Lett.* **95**(22), 225507 (2005).
64. G. Zhang, P. Qi, X. Wang, Y. Lu, D. Mann, X. Li, and H. Dai: Hydrogenation and Hydrocarbonation and Etching of Single-Walled Carbon Nanotubes. *J. Am. Chem. Soc.* **128**(18), 6026 (2006).
65. Y. Piao, B. Meany, L. R. Powell, N. Valley, H. Kwon, G. C. Schatz, and Y. Wang: Brightening of carbon nanotube photoluminescence through the incorporation of sp3 defects. *Nat. Chem.* **5**(10), 840 (2013).
66. L. Vaisman, H. D. Wagner, and G. Marom: The role of surfactants in dispersion of carbon nanotubes. *Adv. Colloid Interface Sci.* **128**–**130**, 37 (2006).
67. Y. Tan and D. E. Resasco: Dispersion of Single-Walled Carbon Nanotubes of Narrow Diameter Distribution. *J. Phys. Chem. B* **109**(30), 14454 (2005).
68. M. S. Arnold, A. A. Green, J. F. Hulvat, S. I. Stupp, and M. C. Hersam: Sorting carbon nanotubes by electronic structure using density differentiation. *Nat Nano* **1**(1), 60 (2006).
69. H. Liu, D. Nishide, T. Tanaka, and H. Kataura: Large-scale single-chirality separation of single-wall carbon nanotubes by simple gel chromatography. *Nat. Commun.* **2**, 309 (2011).
70. P. W. Barone, S. Baik, D. A. Heller, and M. S. Strano: Near-infrared optical sensors based on single-walled carbon nanotubes. *Nat Mater* **4**(1), 86 (2005).

71. S. Liu, L. Wei, L. Hao, N. Fang, M. W. Chang, R. Xu, Y. Yang, and Y. Chen: Sharper and Faster "Nano Darts" Kill More Bacteria: A Study of Antibacterial Activity of Individually Dispersed Pristine Single-Walled Carbon Nanotube. *ACS Nano* **3**(12), 3891 (2009).
72. M. Bottini, N. Rosato, and N. Bottini: PEG-Modified Carbon Nanotubes in Biomedicine: Current Status and Challenges Ahead. *Biomacromolecules* **12**(10), 3381 (2011).
73. Z. Liu, X. Sun, N. Nakayama-Ratchford, and H. Dai: Supramolecular Chemistry on Water-Soluble Carbon Nanotubes for Drug Loading and Delivery. *ACS Nano* **1**(1), 50 (2007).
74. Z. Liu, W. Cai, L. He, N. Nakayama, K. Chen, X. Sun, X. Chen, and H. Dai: In vivo biodistribution and highly efficient tumour targeting of carbon nanotubes in mice. *Nat. Nanotechnol.* **2**(1), 47 (2007).
75. K. Welsher, Z. Liu, S. P. Sherlock, J. T. Robinson, Z. Chen, D. Daranciang, and H. Dai: A route to brightly fluorescent carbon nanotubes for near-infrared imaging in mice. *Nat Nano* **4**(11), 773 (2009).
76. K. Welsher, S. P. Sherlock, and H. Dai: Deep-tissue anatomical imaging of mice using carbon nanotube fluorophores in the second near-infrared window. *Proc. Natl. Acad. Sci.* **108**(22), 8943 (2011).
77. G. Hong, S. Diao, J. Chang, A. L. Antaris, C. Chen, B. Zhang, S. Zhao, D. N. Atochin, P. L. Huang, K. I. Andreasson, C. J. Kuo, and H. Dai: Through-skull fluorescence imaging of the brain in a new near-infrared window. *Nat. Photonics* **8**(9), 723 (2014).
78. G. Hong, J. C. Lee, J. T. Robinson, U. Raaz, L. Xie, N. F. Huang, J. P. Cooke, and H. Dai: Multifunctional in vivo vascular imaging using near-infrared II fluorescence. *Nat. Med.* **18**(12), 1841 (2012).
79. A. L. Antaris, J. T. Robinson, O. K. Yaghi, G. Hong, S. Diao, R. Luong, and H. Dai: Ultra-Low Doses of Chirality Sorted (6,5) Carbon Nanotubes for Simultaneous Tumor Imaging and Photothermal Therapy. *ACS Nano* **7**(4), 3644 (2013).
80. H. Yi, D. Ghosh, M.-H. Ham, J. Qi, P. W. Barone, M. S. Strano, and A. M. Belcher: M13 Phage-Functionalized Single-Walled Carbon Nanotubes As Nanoprobes for Second Near-Infrared Window Fluorescence Imaging of Targeted Tumors. *Nano Lett* **12**(3), 1176 (2012).
81. D. Ghosh, A. F. Bagley, Y. J. Na, M. J. Birrer, S. N. Bhatia, and A. M. Belcher: Deep, noninvasive imaging and surgical guidance of submillimeter tumors using targeted M13-stabilized single-walled carbon nanotubes. *Proc. Natl. Acad. Sci.* 201400821 (2014).
82. N. M. Bardhan, D. Ghosh, and A. M. Belcher: Carbon nanotubes as in vivo bacterial probes. *Nat. Commun.* **5**, 4918 (2014).
83. A. N. Enyashin, S. Gemming, and G. Seifert: DNA-wrapped carbon nanotubes. *Nanotechnology* **18**(24), 245702 (2007).
84. M. Zheng, A. Jagota, E. D. Semke, B. A. Diner, R. S. Mclean, S. R. Lustig, R. E. Richardson, and N. G. Tassi: DNA-assisted dispersion and separation of carbon nanotubes. *Nat Mater* **2**(5), 338 (2003).
85. M. Zheng, A. Jagota, M. S. Strano, A. P. Santos, P. Barone, S. G. Chou, B. A. Diner, M. S. Dresselhaus, R. S. Mclean, G. B. Onoa, G. G. Samsonidze, E. D. Semke, M. Usrey, and D. J. Walls: Structure-Based Carbon Nanotube Sorting by Sequence-Dependent DNA Assembly. *Science* **302**(5650), 1545 (2003).

86. M. S. Strano, M. Zheng, A. Jagota, G. B. Onoa, D. A. Heller, P. W. Barone, and M. L. Usrey: Understanding the Nature of the DNA-Assisted Separation of Single-Walled Carbon Nanotubes Using Fluorescence and Raman Spectroscopy. *Nano Lett.* **4**(4), 543 (2004).
87. M. Zheng and E. D. Semke: Enrichment of Single Chirality Carbon Nanotubes. *J. Am. Chem. Soc.* **129**(19), 6084 (2007).
88. N. M. Iverson, P. W. Barone, M. Shandell, L. J. Trudel, S. Sen, F. Sen, V. Ivanov, E. Atolia, E. Farias, T. P. McNicholas, N. Reuel, N. M. A. Parry, G. N. Wogan, and M. S. Strano: In vivo biosensing via tissue-localizable near-infrared-fluorescent single-walled carbon nanotubes. *Nat. Nanotechnol.* **8**(11), 873 (2013).
89. J.-H. Kim, D. A. Heller, H. Jin, P. W. Barone, C. Song, J. Zhang, L. J. Trudel, G. N. Wogan, S. R. Tannenbaum, and M. S. Strano: The rational design of nitric oxide selectivity in single-walled carbon nanotube near-infrared fluorescence sensors for biological detection. *Nat. Chem.* **1**(6), 473 (2009).
90. N. M. Iverson, G. Bisker, E. Farias, V. Ivanov, J. Ahn, G. N. Wogan, and M. S. Strano: Quantitative Tissue Spectroscopy of Near Infrared Fluorescent Nanosensor Implants. *J. Biomed. Nanotechnol.* **12**(5), 1035 (2016).
91. J. P. Giraldo, M. P. Landry, S. M. Faltermeier, T. P. McNicholas, N. M. Iverson, A. A. Boghossian, N. F. Reuel, A. J. Hilmer, F. Sen, J. A. Brew, and M. S. Strano: Plant nanobionics approach to augment photosynthesis and biochemical sensing. *Nat. Mater.* **13**(4), 400 (2014).
92. I. Kumar, S. Rana, and J. W. Cho: Cycloaddition Reactions: A Controlled Approach for Carbon Nanotube Functionalization. *Chem. – Eur. J.* **17**(40), 11092 (2011).
93. C. Klumpp, K. Kostarelos, M. Prato, and A. Bianco: Functionalized carbon nanotubes as emerging nanovectors for the delivery of therapeutics. *Biochim. Biophys. Acta BBA - Biomembr.* **1758**(3), 404 (2006).
94. X. Zhang, L. Meng, Q. Lu, Z. Fei, and P. J. Dyson: Targeted delivery and controlled release of doxorubicin to cancer cells using modified single wall carbon nanotubes. *Biomaterials* **30**(30), 6041 (2009).
95. N. W. S. Kam, M. O'Connell, J. A. Wisdom, and H. Dai: Carbon nanotubes as multifunctional biological transporters and near-infrared agents for selective cancer cell destruction. *Proc. Natl. Acad. Sci. U. S. A.* **102**(33), 11600 (2005).
96. S. Fedeli, A. Brandi, L. Venturini, P. Chiarugi, E. Giannoni, P. Paoli, D. Corti, G. Giambastiani, G. Tuci, and S. Cicchi: The "click-on-tube" approach for the production of efficient drug carriers based on oxidized multi-walled carbon nanotubes. *J. Mater. Chem. B* **4**(21), 3823 (2016).
97. M. Pescatori, D. Bedognetti, E. Venturelli, C. Ménard-Moyon, C. Bernardini, E. Muresu, A. Piana, G. Maida, R. Manetti, F. Sgarrella, A. Bianco, and L. G. Delogu: Functionalized carbon nanotubes as immunomodulator systems. *Biomaterials* **34**(18), 4395 (2013).
98. P. C. B. de Faria, L. I. dos Santos, J. P. Coelho, H. B. Ribeiro, M. A. Pimenta, L. O. Ladeira, D. A. Gomes, C. A. Furtado, and R. T. Gazzinelli: Oxidized Multiwalled Carbon Nanotubes as Antigen Delivery System to Promote Superior CD8+ T Cell Response and Protection against Cancer. *Nano Lett.* **14**(9), 5458 (2014).
99. X. An, T. W. Butler, M. Washington, S. K. Nayak, and S. Kar: Optical and Sensing Properties of 1-Pyrenecarboxylic Acid-Functionalized Graphene Films Laminated on Polydimethylsiloxane Membranes. *ACS Nano* **5**(2), 1003 (2011).

100. Y. Xu, H. Bai, G. Lu, C. Li, and G. Shi: Flexible Graphene Films via the Filtration of Water-Soluble Noncovalent Functionalized Graphene Sheets. *J. Am. Chem. Soc.* **130**(18), 5856 (2008).
101. Y. Wang, X. Chen, Y. Zhong, F. Zhu, and K. P. Loh: Large area, continuous, few-layered graphene as anodes in organic photovoltaic devices. *Appl. Phys. Lett.* **95**(6), 63302 (2009).
102. V. K. Kodali, J. Scrimgeour, S. Kim, J. H. Hankinson, K. M. Carroll, W. A. de Heer, C. Berger, and J. E. Curtis: Nonperturbative Chemical Modification of Graphene for Protein Micropatterning. *Langmuir* **27**(3), 863 (2011).
103. Y. Liu, L. Yuan, M. Yang, Y. Zheng, L. Li, L. Gao, N. Nerngchamnong, C. T. Nai, C. S. S. Sangeeth, Y. P. Feng, C. A. Nijhuis, and K. P. Loh: Giant enhancement in vertical conductivity of stacked CVD graphene sheets by self-assembled molecular layers. *Nat. Commun.* **5**, 5461 (2014).
104. Q. Su, S. Pang, V. Alijani, C. Li, X. Feng, and K. Müllen: Composites of Graphene with Large Aromatic Molecules. *Adv. Mater.* **21**(31), 3191 (2009).
105. H.-C. Cheng, R.-J. Shiue, C.-C. Tsai, W.-H. Wang, and Y.-T. Chen: High-Quality Graphene p−n Junctions via Resist-free Fabrication and Solution-Based Noncovalent Functionalization. *ACS Nano* **5**(3), 2051 (2011).
106. K. D. Papadimitriou, E. N. Skountzos, S. S. Gkermpoura, I. Polyzos, V. G. Mavrantzas, C. Galiotis, and C. Tsitsilianis: Molecular Modeling Combined with Advanced Chemistry for the Rational Design of Efficient Graphene Dispersing Agents. *ACS Macro Lett.* **5**(1), 24 (2016).
107. X. Wang, S. M. Tabakman, and H. Dai: Atomic Layer Deposition of Metal Oxides on Pristine and Functionalized Graphene. *J. Am. Chem. Soc.* **130**(26), 8152 (2008).
108. Q. H. Wang and M. C. Hersam: Room-temperature molecular-resolution characterization of self-assembled organic monolayers on epitaxial graphene. *Nat. Chem.* **1**(3), 206 (2009).
109. N. V. Kozhemyakina, J. M. Englert, G. Yang, E. Spiecker, C. D. Schmidt, F. Hauke, and A. Hirsch: Non-Covalent Chemistry of Graphene: Electronic Communication with Dendronized Perylene Bisimides. *Adv. Mater.* **22**(48), 5483 (2010).
110. W. Tu, J. Lei, S. Zhang, and H. Ju: Characterization, Direct Electrochemistry, and Amperometric Biosensing of Graphene by Noncovalent Functionalization with Picket-Fence Porphyrin. *Chem. – Eur. J.* **16**(35), 10771 (2010).
111. J. Geng and H.-T. Jung: Porphyrin Functionalized Graphene Sheets in Aqueous Suspensions: From the Preparation of Graphene Sheets to Highly Conductive Graphene Films. *J. Phys. Chem. C* **114**(18), 8227 (2010).
112. S. Zhang, S. Tang, J. Lei, H. Dong, and H. Ju: Functionalization of graphene nanoribbons with porphyrin for electrocatalysis and amperometric biosensing. *J. Electroanal. Chem.* **656**(1–2), 285 (2011).
113. J. O. Sofo, A. S. Chaudhari, and G. D. Barber: Graphane: A two-dimensional hydrocarbon. *Phys. Rev. B* **75**(15), 153401 (2007).
114. D. C. Elias, R. R. Nair, T. M. G. Mohiuddin, S. V. Morozov, P. Blake, M. P. Halsall, A. C. Ferrari, D. W. Boukhvalov, M. I. Katsnelson, A. K. Geim, and K. S. Novoselov: Control of Graphene's Properties by Reversible Hydrogenation: Evidence for Graphane. *Science* **323**(5914), 610 (2009).
115. S. Ryu, M. Y. Han, J. Maultzsch, T. F. Heinz, P. Kim, M. L. Steigerwald, and L. E. Brus: Reversible Basal Plane Hydrogenation of Graphene. *Nano Lett.* **8**(12), 4597 (2008).

116. H. Sahin, O. Leenaerts, S. K. Singh, and F. M. Peeters: Graphane. *Wiley Interdiscip. Rev. Comput. Mol. Sci.* **5**(3), 255 (2015).
117. S. M. Tan, Z. Sofer, and M. Pumera: Biomarkers Detection on Hydrogenated Graphene Surfaces: Towards Applications of Graphane in Biosensing. *Electroanalysis* **25**(3), 703 (2013).
118. R. R. Nair, W. Ren, R. Jalil, I. Riaz, V. G. Kravets, L. Britnell, P. Blake, F. Schedin, A. S. Mayorov, S. Yuan, M. I. Katsnelson, H.-M. Cheng, W. Strupinski, L. G. Bulusheva, A. V. Okotrub, I. V. Grigorieva, A. N. Grigorenko, K. S. Novoselov, and A. K. Geim: Fluorographene: A Two-Dimensional Counterpart of Teflon. *Small* **6**(24), 2877 (2010).
119. J. T. Robinson, J. S. Burgess, C. E. Junkermeier, S. C. Badescu, T. L. Reinecke, F. K. Perkins, M. K. Zalalutdniov, J. W. Baldwin, J. C. Culbertson, P. E. Sheehan, and E. S. Snow: Properties of Fluorinated Graphene Films. *Nano Lett.* **10**(8), 3001 (2010).
120. F. Karlický, R. Zbořil, and M. Otyepka: Band gaps and structural properties of graphene halides and their derivates: A hybrid functional study with localized orbital basis sets. *J. Chem. Phys.* **137**(3), 34709 (2012).
121. R. Zbořil, F. Karlický, A. B. Bourlinos, T. A. Steriotis, A. K. Stubos, V. Georgakilas, K. Šafářová, D. Jančík, C. Trapalis, and M. Otyepka: Graphene Fluoride: A Stable Stoichiometric Graphene Derivative and its Chemical Conversion to Graphene. *Small* **6**(24), 2885 (2010).
122. A. B. Bourlinos, K. Safarova, K. Siskova, and R. Zbořil: The production of chemically converted graphenes from graphite fluoride. *Carbon* **50**(3), 1425 (2012).
123. S. Park and R. S. Ruoff: Chemical methods for the production of graphenes. *Nat. Nanotechnol.* **4**(4), 217 (2009).
124. M. Quintana, K. Spyrou, M. Grzelczak, W. R. Browne, P. Rudolf, and M. Prato: Functionalization of Graphene via 1,3-Dipolar Cycloaddition. *ACS Nano* **4**(6), 3527 (2010).
125. L.-H. Liu, M. M. Lerner, and M. Yan: Derivitization of Pristine Graphene with Well-Defined Chemical Functionalities. *Nano Lett.* **10**(9), 3754 (2010).
126. J. Choi, K. Kim, B. Kim, H. Lee, and S. Kim: Covalent Functionalization of Epitaxial Graphene by Azidotrimethylsilane. *J. Phys. Chem. C* **113**(22), 9433 (2009).
127. H. He and C. Gao: General Approach to Individually Dispersed, Highly Soluble, and Conductive Graphene Nanosheets Functionalized by Nitrene Chemistry. *Chem. Mater.* **22**(17), 5054 (2010).
128. X. Zhong, J. Jin, S. Li, Z. Niu, W. Hu, R. Li, and J. Ma: Aryne cycloaddition: highly efficient chemical modification of graphene. *Chem. Commun.* **46**(39), 7340 (2010).
129. M. Wu, R. Kempaiah, P.-J. J. Huang, V. Maheshwari, and J. Liu: Adsorption and Desorption of DNA on Graphene Oxide Studied by Fluorescently Labeled Oligonucleotides. *Langmuir* **27**(6), 2731 (2011).
130. J. M. Yun, K. N. Kim, J. Y. Kim, D. O. Shin, W. J. Lee, S. H. Lee, M. Lieberman, and S. O. Kim: DNA Origami Nanopatterning on Chemically Modified Graphene. *Angew. Chem. Int. Ed.* **51**(4), 912 (2012).
131. N. Mohanty and V. Berry: Graphene-Based Single-Bacterium Resolution Biodevice and DNA Transistor: Interfacing Graphene Derivatives with Nanoscale and Microscale Biocomponents. *Nano Lett.* **8**(12), 4469 (2008).

132. J. Liu, Y. Li, Y. Li, J. Li, and Z. Deng: Noncovalent DNA decorations of graphene oxide and reduced graphene oxide toward water -soluble metal– carbon hybrid nanostructures via self-assembly. *J. Mater. Chem.* **20**(5), 900 (2010).
133. C.-H. Lu, H.-H. Yang, C.-L. Zhu, X. Chen, and G.-N. Chen: A Graphene Platform for Sensing Biomolecules. *Angew. Chem. Int. Ed.* **48**(26), 4785 (2009).
134. Y. Xu, Q. Wu, Y. Sun, H. Bai, and G. Shi: Three-Dimensional Self-Assembly of Graphene Oxide and DNA into Multifunctional Hydrogels. *ACS Nano* **4**(12), 7358 (2010).
135. S. J. Heerema and C. Dekker: Graphene nanodevices for DNA sequencing. *Nat. Nanotechnol.* **11**(2), 127 (2016).
136. D. R. Dreyer, S. Park, C. W. Bielawski, and R. S. Ruoff: The chemistry of graphene oxide. *Chem. Soc. Rev.* **39**(1), 228 (2009).
137. J. T. Robinson, S. M. Tabakman, Y. Liang, H. Wang, H. Sanchez Casalongue, D. Vinh, and H. Dai: Ultrasmall Reduced Graphene Oxide with High Near-Infrared Absorbance for Photothermal Therapy. *J. Am. Chem. Soc.* **133**(17), 6825 (2011).
138. H. J. Yoon, T. H. Kim, Z. Zhang, E. Azizi, T. M. Pham, C. Paoletti, J. Lin, N. Ramnath, M. S. Wicha, D. F. Hayes, D. M. Simeone, and S. Nagrath: Sensitive capture of circulating tumour cells by functionalized graphene oxide nanosheets. *Nat. Nanotechnol.* **8**(10), 735 (2013).
139. H. J. Yoon, A. Shanker, Y. Wang, M. Kozminsky, Q. Jin, N. Palanisamy, M. L. Burness, E. Azizi, D. M. Simeone, M. S. Wicha, J. Kim, and S. Nagrath: Tunable Thermal-Sensitive Polymer–Graphene Oxide Composite for Efficient Capture and Release of Viable Circulating Tumor Cells. *Adv. Mater.* **28**(24), 4891 (2016).
140. B. Gupta, N. Kumar, K. Panda, A. A. Melvin, S. Joshi, S. Dash, and A. K. Tyagi: Effective Noncovalent Functionalization of Poly(ethylene glycol) to Reduced Graphene Oxide Nanosheets through γ-Radiolysis for Enhanced Lubrication. *J. Phys. Chem. C* **120**(4), 2139 (2016).
141. M. Zhang, Y. Wang, L. Huang, Z. Xu, C. Li, and G. Shi: Multifunctional Pristine Chemically Modified Graphene Films as Strong as Stainless Steel. *Adv. Mater.* **27**(42), 6708 (2015).
142. Q. Liu, M. Zhang, L. Huang, Y. Li, J. Chen, C. Li, and G. Shi: High-Quality Graphene Ribbons Prepared from Graphene Oxide Hydrogels and Their Application for Strain Sensors. *ACS Nano* **9**(12), 12320 (2015).
143. A. Servant, A. Bianco, M. Prato, and K. Kostarelos: Graphene for multi-functional synthetic biology: The last "zeitgeist" in nanomedicine. *Bioorg. Med. Chem. Lett.* **24**(7), 1638 (2014).
144. S. Niyogi, E. Bekyarova, M. E. Itkis, H. Zhang, K. Shepperd, J. Hicks, M. Sprinkle, C. Berger, C. N. Lau, W. A. deHeer, E. H. Conrad, and R. C. Haddon: Spectroscopy of Covalently Functionalized Graphene. *Nano Lett.* **10**(10), 4061 (2010).
145. L. Zhang, J. Xia, Q. Zhao, L. Liu, and Z. Zhang: Functional Graphene Oxide as a Nanocarrier for Controlled Loading and Targeted Delivery of Mixed Anticancer Drugs. *Small* **6**(4), 537 (2010).
146. G. Wei, M. Yan, R. Dong, D. Wang, X. Zhou, J. Chen, and J. Hao: Covalent Modification of Reduced Graphene Oxide by Means of Diazonium Chemistry and Use as a Drug-Delivery System. *Chem. – Eur. J.* **18**(46), 14708 (2012).

147. G. Gollavelli and Y.-C. Ling: Multi-functional graphene as an in vitro and in vivo imaging probe. *Biomaterials* **33**(8), 2532 (2012).
148. Z. Liu, J. T. Robinson, X. Sun, and H. Dai: PEGylated Nanographene Oxide for Delivery of Water-Insoluble Cancer Drugs. *J. Am. Chem. Soc.* **130**(33), 10876 (2008).
149. K. Yang, S. Zhang, G. Zhang, X. Sun, S.-T. Lee, and Z. Liu: Graphene in Mice: Ultrahigh In Vivo Tumor Uptake and Efficient Photothermal Therapy. *Nano Lett.* **10**(9), 3318 (2010).
150. W. Zhang, Z. Guo, D. Huang, Z. Liu, X. Guo, and H. Zhong: Synergistic effect of chemo-photothermal therapy using PEGylated graphene oxide. *Biomaterials* **32**(33), 8555 (2011).
151. B. Tian, C. Wang, S. Zhang, L. Feng, and Z. Liu: Photothermally Enhanced Photodynamic Therapy Delivered by Nano-Graphene Oxide. *ACS Nano* **5**(9), 7000 (2011).
152. J. Cao, H. An, X. Huang, G. Fu, R. Zhuang, L. Zhu, J. Xie, and F. Zhang: Monitoring of the tumor response to nano-graphene oxide-mediated photothermal/photodynamic therapy by diffusion-weighted and BOLD MRI. *Nanoscale* **8**(19), 10152 (2016).
153. L. Feng, X. Yang, X. Shi, X. Tan, R. Peng, J. Wang, and Z. Liu: Polyethylene Glycol and Polyethylenimine Dual-Functionalized Nano-Graphene Oxide for Photothermally Enhanced Gene Delivery. *Small* **9**(11), 1989 (2013).
154. C. Shan, H. Yang, D. Han, Q. Zhang, A. Ivaska, and L. Niu: Water-Soluble Graphene Covalently Functionalized by Biocompatible Poly-l-lysine. *Langmuir* **25**(20), 12030 (2009).
155. H. Hong, K. Yang, Y. Zhang, J. W. Engle, L. Feng, Y. Yang, T. R. Nayak, S. Goel, J. Bean, C. P. Theuer, T. E. Barnhart, Z. Liu, and W. Cai: In Vivo Targeting and Imaging of Tumor Vasculature with Radiolabeled, Antibody-Conjugated Nanographene. *ACS Nano* **6**(3), 2361 (2012).
156. G.-Y. Chen, Z. Li, C. S. Theile, N. M. Bardhan, P. V. Kumar, J. N. Duarte, T. Maruyama, A. Rashidfarrokh, A. M. Belcher, and H. L. Ploegh: Graphene Oxide Nanosheets Modified with Single-Domain Antibodies for Rapid and Efficient Capture of Cells. *Chem. – Eur. J.* **21**(48), 17178 (2015).
157. C. M. Sayes, F. Liang, J. L. Hudson, J. Mendez, W. Guo, J. M. Beach, V. C. Moore, C. D. Doyle, J. L. West, W. E. Billups, K. D. Ausman, and V. L. Colvin: Functionalization density dependence of single-walled carbon nanotubes cytotoxicity in vitro. *Toxicol. Lett.* **161**(2), 135 (2006).
158. F. Zhao, H. Meng, L. Yan, B. Wang, and Y. Zhao: Nanosurface chemistry and dose govern the bioaccumulation and toxicity of carbon nanotubes, metal nanomaterials and quantum dots in vivo. *Sci. Bull.* **60**(1), 3 (2014).
159. Q. Mu, G. Su, L. Li, B. O. Gilbertson, L. H. Yu, Q. Zhang, Y.-P. Sun, and B. Yan: Size-Dependent Cell Uptake of Protein-Coated Graphene Oxide Nanosheets. *ACS Appl. Mater. Interfaces* **4**(4), 2259 (2012).
160. G. Jia, H. Wang, L. Yan, X. Wang, R. Pei, T. Yan, Y. Zhao, and X. Guo: Cytotoxicity of Carbon Nanomaterials: Single-Wall Nanotube, Multi-Wall Nanotube, and Fullerene. *Environ. Sci. Technol.* **39**(5), 1378 (2005).
161. S. K. Manna, S. Sarkar, J. Barr, K. Wise, E. V. Barrera, O. Jejelowo, A. C. Rice-Ficht, and G. T. Ramesh: Single-Walled Carbon Nanotube Induces Oxidative Stress and Activates Nuclear Transcription Factor-κB in Human Keratinocytes. *Nano Lett.* **5**(9), 1676 (2005).

162. K. Kostarelos, L. Lacerda, G. Pastorin, W. Wu, S. Wieckowski, J. Luangsivilay, S. Godefroy, D. Pantarotto, J.-P. Briand, S. Muller, M. Prato, and A. Bianco: Cellular uptake of functionalized carbon nanotubes is independent of functional group and cell type. *Nat. Nanotechnol.* **2**(2), 108 (2007).
163. X. Hu, S. Cook, P. Wang, H. Hwang, X. Liu, and Q. L. Williams: In vitro evaluation of cytotoxicity of engineered carbon nanotubes in selected human cell lines. *Sci. Total Environ.* **408**(8), 1812 (2010).
164. S. Arora, H. Kaur, R. Kumar, R. Kaur, D. Rana, C. S. Rayat, I. Kaur, S. K. Arora, P. Bubber, and L. M. Bharadwaj: In Vitro Cytotoxicity of Multiwalled and Single-Walled Carbon Nanotubes on Human Cell Lines. *Fuller. Nanotub. Carbon Nanostructures* **23**(5), 377 (2015).
165. D. Breznan, D. Das, C. MacKinnon-Roy, B. Simard, P. Kumarathasan, and R. Vincent: Non-specific interaction of carbon nanotubes with the resazurin assay reagent: Impact on in vitro assessment of nanoparticle cytotoxicity. *Toxicol. In Vitro* **29**(1), 142 (2015).
166. P. Cherukuri, S. M. Bachilo, S. H. Litovsky, and R. B. Weisman: Near-Infrared Fluorescence Microscopy of Single-Walled Carbon Nanotubes in Phagocytic Cells. *J. Am. Chem. Soc.* **126**(48), 15638 (2004).
167. K. P. Loh, Q. Bao, G. Eda, and M. Chhowalla: Graphene oxide as a chemically tunable platform for optical applications. *Nat. Chem.* **2**(12), 1015 (2010).
168. K.-H. Liao, Y.-S. Lin, C. W. Macosko, and C. L. Haynes: Cytotoxicity of Graphene Oxide and Graphene in Human Erythrocytes and Skin Fibroblasts. *ACS Appl. Mater. Interfaces* **3**(7), 2607 (2011).
169. Y. Chang, S.-T. Yang, J.-H. Liu, E. Dong, Y. Wang, A. Cao, Y. Liu, and H. Wang: In vitro toxicity evaluation of graphene oxide on A549 cells. *Toxicol. Lett.* **200**(3), 201 (2011).
170. W. Hu, C. Peng, M. Lv, X. Li, Y. Zhang, N. Chen, C. Fan, and Q. Huang: Protein Corona-Mediated Mitigation of Cytotoxicity of Graphene Oxide. *ACS Nano* **5**(5), 3693 (2011).
171. X. Sun, Z. Liu, K. Welsher, J. T. Robinson, A. Goodwin, S. Zaric, and H. Dai: Nano-graphene oxide for cellular imaging and drug delivery. *Nano Res.* **1**(3), 203 (2008).
172. K. Yang, J. Wan, S. Zhang, Y. Zhang, S.-T. Lee, and Z. Liu: In Vivo Pharmacokinetics, Long-Term Biodistribution, and Toxicology of PEGylated Graphene in Mice. *ACS Nano* **5**(1), 516 (2011).
173. M. L. Schipper, N. Nakayama-Ratchford, C. R. Davis, N. W. S. Kam, P. Chu, Z. Liu, X. Sun, H. Dai, and S. S. Gambhir: A pilot toxicology study of single-walled carbon nanotubes in a small sample of mice. *Nat Nano* **3**(4), 216 (2008).
174. M. Kryuchkova, A. Danilushkina, Y. Lvov, and R. Fakhrullin: Evaluation of toxicity of nanoclays and graphene oxide in vivo: a Paramecium caudatum study. *Environ. Sci. Nano* **3**(2), 442 (2016).
175. C. P. Firme III and P. R. Bandaru: Toxicity issues in the application of carbon nanotubes to biological systems. *Nanomedicine Nanotechnol. Biol. Med.* **6**(2), 245 (2010).
176. R. Singh, D. Pantarotto, L. Lacerda, G. Pastorin, C. Klumpp, M. Prato, A. Bianco, and K. Kostarelos: Tissue biodistribution and blood clearance rates of intravenously administered carbon nanotube radiotracers. *Proc. Natl. Acad. Sci. U. S. A.* **103**(9), 3357 (2006).

177. Z. Liu, C. Davis, W. Cai, L. He, X. Chen, and H. Dai: Circulation and long-term fate of functionalized, biocompatible single-walled carbon nanotubes in mice probed by Raman spectroscopy. *Proc. Natl. Acad. Sci.* **105**(5), 1410 (2008).
178. J. T. Robinson, G. Hong, Y. Liang, B. Zhang, O. K. Yaghi, and H. Dai: In Vivo Fluorescence Imaging in the Second Near-Infrared Window with Long Circulating Carbon Nanotubes Capable of Ultrahigh Tumor Uptake. *J Am Chem Soc* **134**(25), 10664 (2012).
179. Y. Liu, Y. Luo, J. Wu, Y. Wang, X. Yang, R. Yang, B. Wang, J. Yang, and N. Zhang: Graphene oxide can induce in vitro and in vivo mutagenesis. *Sci. Rep.* **3**, 3469 (2013).
180. S. Zhang, K. Yang, L. Feng, and Z. Liu: In vitro and in vivo behaviors of dextran functionalized graphene. *Carbon* **49**(12), 4040 (2011).
181. K. Yang, H. Gong, X. Shi, J. Wan, Y. Zhang, and Z. Liu: In vivo biodistribution and toxicology of functionalized nano-graphene oxide in mice after oral and intraperitoneal administration. *Biomaterials* **34**(11), 2787 (2013).
182. S. K. Singh, M. K. Singh, P. P. Kulkarni, V. K. Sonkar, J. J. A. Grácio, and D. Dash: Amine-Modified Graphene: Thrombo-Protective Safer Alternative to Graphene Oxide for Biomedical Applications. *ACS Nano* **6**(3), 2731 (2012).
183. G. Lalwani and B. Sitharaman: Multifunctional fullerene- and metallofullerene-based nanobiomaterials. *Nano LIFE* **3**(3), 1342003 (2013).
184. B. S. Harrison and A. Atala: Carbon nanotube applications for tissue engineering. *Biomaterials* **28**(2), 344 (2007).
185. A. B. Seabra, A. J. Paula, R. de Lima, O. L. Alves, and N. Durán: Nanotoxicity of Graphene and Graphene Oxide. *Chem. Res. Toxicol.* **27**(2), 159 (2014).